DESIGN OF A VIBROTACTILE BALANCE SUPPORT SYSTEM WITH A VIRTUAL REALITY TRAINING PROGRAM

by

ENES TARIK ARAS

B.S., in Electrical and Electronics Engineering, İstanbul Şehir University, 2019

Submitted to the Institute of Biomedical Engineering
in partial fulfillment of the requirements
for the degree of
Master of Science
in
Biomedical Engineering

Boğaziçi University
2022

ACKNOWLEDGMENTS

First, I would like to thank my thesis supervisor and my mentor Prof. Dr. Burak GÜÇLÜ, for his guidance and support. Also, I would like to thank Prof. Dr. Albert GÜVENİŞ and Assoc Prof. Mustafa Zahid YILDIZ for their valuable contributions.

I want to thank my family for always being there for me. Finally, I want to thank my supportive friends Kutluhan MAHMAT and İsmail ERBAŞ for their supportive comments and endless friendship.

ACADEMIC ETHICS AND INTEGRITY STATEMENT

I, Enes Tarık ARAS, hereby certify that I am aware of the Academic Ethics and Integrity Policy issued by the Council of Higher Education (YÖK) and I fully acknowledge all the consequences due to its violation by plagiarism or any other way.

Name :

Signature:

Date:

ABSTRACT

DESIGN OF A VIBROTACTILE BALANCE SUPPORT SYSTEM WITH A VIRTUAL REALITY TRAINING PROGRAM

This thesis aims to design a vibrotactile feedback(VTF) system to help balance rehabilitation with virtual reality (VR) training. First, the training program was built in a virtual reality platform by using Unity3D and Blender software. Data for visual and vibrotactile psychophysical limits were obtained in several experiments performed by one participant. The VR platform simulated anterior/posterior sways which were conveyed to the participant visually and/or by VTF. Visual experiments consisted of motion detection, angle discrimination, and angular velocity discrimination of an avatar in the VR screen. All motion detection thresholds were found to be lower than 0.04 deg/s. Angle and velocity discrimination limens were in the range of 0.26-0.46 deg and 0.19-0.34 deg/s in the visual avatar. Arduino UNO was used to control six vibration motors placed around the upper arm . Motors were recruited incrementally as the avatar's sway angle increased. Angular velocity was mapped either by mixed (Pulse-width/pulse-number) or pulse-number modulation to the VTF. Motor distances were adjusted to ensure maximum (%81.2) localization. Next, the participant matched VTF to the postural sway of the avatar while the computer screen was off. Combined identification accuracy of sway angle and angular velocity was 91% by only VTF. Finally, the avatar was simulated to cross a road in the VR platform with three conditions (visual on tactile off, visual off tactile on, visual on tactile on) participant. In all conditions, the participant could control the avatar successfully without any falls. Quickest response was obtained when both feedbacks were on (98.7%), and the worst response was obtained when only VTF was on (92.1%). VTF seems promising in the proof of concept balance support system presented in this thesis.

Keywords: Somatosensory Feedback, Tactile Sensor, Proprioceptive Sensor, Touch, Arduino, Virtual Reality, Augmented Reality, Vestibular System, Balance, Posture, Balance Disorder, Postural Sway, Center of Mass, Center of Pressure, Limit of Stability.

ÖZET

SANAL GERÇEKLİK EĞİTİM PROGRAMI İÇEREN BİR VİBROTAKTİL DENGE DESTEK SİSTEMİNİN TASARIMI

Bu tezde denge rehabilitasyonuna yardımcı olabilmek için sanal gerçeklik (SG) eğitimi ile vibrotaktil geri bildirim (VGB) sistemi tasarlanması amaçlanmıştır. Eğitim programı Unity3D ve Blender yazılımları üzerine kurulmuştur. Görsel ve vibrotaktil psikofiziksel limitler bir katılımcı yardımıyla deneylerde ölçülmüştür. Anterior/posterior salınımlarla ilgili bilgi görsel ve/veya VGB ile katılımcıya aktarılmıştır. Görsel deneyler, avatar üzerinden SG'de hareket algılama, açı ve hız diskriminasyonu testlerini kapsamaktadır. Hareket algılamada bütün eşik değerleri 0.04 deg/s'nin altındadır. Görüntülenen avatarın açı ve hız diskriminasyonu eşik değerleri ise 0.26-0.46 deg ve 0.19-0.34 deg aralığında bulunmuştur. VGB için Arduino UNO kullanılarak üst kola yerleştirilen altı motor sürülmüştür. Avatarın artan açısı ile eş çalıştırılan motor sayısı arttırılmıştır. Avatarın açısal hızı ise karışık (darbe genişliği/darbe sayısı) ya da darbe sayısı modülasyonu ile VGB'ye dönüştürülmüştür. Motorlar arası mesafe maksimum lokalizasyon doğruluğuna (%81.2) ulaşılacak şekilde ayarlanmıştır. Katılımcı VGB'yi ekran kapalıyken avatarın postural salınımlarına eşleştirmiştir. Sadece VGB ile elde edilen birleştirilmiş salınım açısı ve hızı doğruluk %91 bulunmuştur. Son olarak avatar, katılımcının üç farklı durumunda (gözler açık VGB kapalı, gözler kapalı VGB açık, gözler açık VGB açık) bir yolda karşıdan karşıya geçmesi için simüle edilmiştir. Bütün durumlarda katılımcı avatarı hiç düşürmeden kontrol edebilmiştir. En iyi performans (%98.7) iki modalitede geribildirim varken, en kötü performans (%92.1) ise sadece VGB açıkken ölçülmüştür. VGB kullanılarak tasarlanan denge destek sistemi klinik çalışmalar için umut vermektedir.

Anahtar Kelimeler: Vibrotaktil Geri Bildirim, Dokunma, Arduino, Sanal Gerçeklik, Arttırılmış Gerçeklik, Vestibular Sistem, Denge, Postür, Denge Bozuklukları, Postüral Salınım, Kütle Merkezi, Basınç Merkezi, Stabilite Limiti.

TABLE OF CONTENTS

LIST OF FIGURES

LIST OF TABLES

LIST OF SYMBOLS

Fx	Horizontal Force
Fy	Vertical Force
mg	Acceleration of the gravity
Θmax	Maximum Rotation Angle
Θmin	Minimum Rotation Angle

LIST OF ABBREVIATIONS

ABC	Activated-Specific Balance Confidence Scale
TUG	Time Up and Go
BESTest	The Balance Evaluation Test
COP	Center of pressure
COM	Center of Mass
COG	Center of Gravity
CDP	Computerized Dynamic Posturography
SOT	Sensory Organization Test
S2	Second vertebrae of sacral
3D	Three Dimensional
VR	Virtual Reality
AR	Augmented Reality
HMD	Head-mounted Display
CT	Computed Tomography
APL	Arduino programming language
IDE	Integrated Development Environment
ERM	Eccentric Rotating Mass vibration motor
AREM	Anterior Rotation Encoding Motor
PREM	Posterior Rotation Encoding Motor

1. INTRODUCTION

1.1 Motivation and Aim

Balance and postural control disorders are widespread problems caused by various neurological and vestibular diseases that significantly reduce the life quality of patients. At least 2 million people in the USA suffer from chronic balance disorders. [1]. Most daily life activities depend on postural control and equilibrium. For example, while taking a walk in a park or sitting on a chair in a coffee, multiple sensory systems provide postural information. Any disturbance in one of the relevant sensory systems can cause information loss that affects the balance. Without balance and postural control, those activities cannot be done correctly. Therefore, people with chronic balance disorders need medical attention for balance.

In literature, multiple methods were used to reduce the severity of balance problems. For example, dopaminergic drugs and deep brain stimulations were used to improve the balance of patients with Parkinson's disease [2]. However, with the progression of the disease, those treatments lose their effectiveness. Another approach is wearable balance support systems and balance prostheses that are used to guide the patient by providing information about the current position. Joel A. Goebel et al. showed the effectiveness of vibrotactile feedback for balance guidance by using a head-mounted vibrotactile headset to apply vibrotactile feedback to inform the participant about their posture sway [1]. However, devices like those should be presented with proper training programs to make patients understand how to use the device functionally.

This thesis aims to develop a new balance support device and virtual reality training method for patients with balance and postural control disorders. We designed a virtual environment in Unity 3D to provide configurable visual feedback. In this environment, the participant controlled an avatar designed in Blender software. In

the experiments, the avatar had anterior and posterior sways in different conditions (static/dynamic, standing/walking), and the participant completed tasks according to the conditions. This procedure provides an environment where participants can get pre-training without physical effort. Early experiments were done to collect psychophysical data from the participant to obtain psychophysical limits.

As the balance support device, we designed a special armband with six vibration motors to provide vibrotactile feedback about the patient's anterior-posterior angular position and velocity. Three motors were used to encode the anterior rotation, named Anterior Rotation Encoding Motors (AREM), and the other three for the posterior rotation, called Posterior Rotation Encoding Motors (PREM). Each motor group was placed in a crescent formation on the opposite sides of the armband. Distance between vibration motors was adjustable according to the participant's upper arm circumference. The armband was placed on the upper arm in a circular position as in the previous study by Matthieu Guemann et al [3]. So, we were able to stimulate a sensitive region on the upper arm by not affecting the joint receptors. The armband was connected to a computer through an Arduino UNO microcontroller. Arduino converted the encoded digital signals to voltage signals and activated the motors accordingly. The participant was trained to use the armband. We encoded the specific sway angles and velocities to vibrotactile feedback. The novelties of this study are new encoding and placement methods for vibrotactile feedback and providing a virtual training system that presents third-person observation to participants about their possible sway conditions.

1.2 Outline

The first chapter explains the novelty and needs of this study. Chapter 2 provides essential background information, including balance and postural disorders, vestibular system, somatosensory system, virtual reality, and augmented reality. In chapter 3, materials and methods are explained. In chapter 4, the results of the experiments are presented. The final chapter (chapter 5, discussion) discusses previous studies, technical limitations and some other issues, future work, and a conclusion.

2. BACKGROUND

2.1 Balance and Postural Control Disorders

Balance is the skill of keeping the center of gravity within the limit of stability while stationary or moving. Balance helps people get three abilities: Keeping the posture still, providing safe, voluntary movements, and restoring the loss of balance caused by environmental factors. Balance disorders are common problems caused by neurological or musculoskeletal diseases such as Parkinson's disease, multiple sclerosis, stroke, and vestibular deficit. They can cause falls, limited locomotor functions, and dependency on support equipment. Also, it can bring psychological difficulties like fear of falling or lack of confidence, leading to social isolation. Age is another important factor in balance. People reach their maximum balance performance in early adulthood. However, their balance decreases after their fifties with reduced muscle strength, sensory functioning, and sensory-motor reflexes [4].

Early recognition of balance disorders is essential to identify the patients' fall risk, scale the loss of balance, and develop a particular treatment, rehabilitation, or support strategy. Conducting clinical and instrumental assessments are vital for a detailed diagnosis. Clinical assessment is divided into two sub-groups: functional assessment and system assessment [4]. Functional assessment investigates the existence of any balance disorder and analyses its behavior against external forces if it exists. Six different outcome measures are used to examine balance disorders' functional properties. The Berg Balance Scale (BBS) and the Tinetti Balance and Gait Assessment are classified as rating scales. BBS is a well-established method that supplies a quantitative assessment of balance disorders. It is designed to use on older adults at first. Its effectivity has been investigated in patients with different neurological diseases like PD or vestibular dysfunction. This measure examines the patient's position-keeping skills while decreasing the support base. Another rating scale test is Tinetti Balance and Gait Assessment, also known as the Performance-Oriented Mobility Assessment

(POMA). This test is one of the oldest and most widely used methods to examine balance, gait, and fall risk [5]. The test can be used to examine both balance and gait. The experimenter assesses the balance in four positions: sitting, arising, standing, and turning. Also, some disturbances might be added, and some trials might be run when participants' eyes are closed.

Activated-Specific Balance Confidence Scale (ABC) is a questionnaire type of measure. The experimenter asks the participant to do some daily tasks and answer questions about his performance. According to those answers, he calculates the score of the test. The last three measures are clinical-based tests (Time Up and Go (TUG), One-leg Stance, Functional Reach). TUG is the first clinical and also only time-based test. In that easy experiment, the patient is asked the stand up from a chair, walk 3m to a destination on a particular line at a comfortable speed, turn back to the chair on the same line and sit down on the chair again. The experimenter calculates the trial time and validates the performance accordingly. ("One-leg stance"-"Functional Reach"). These measures have their unique strengths and weaknesses, but they also have common advantages and disadvantages. Procedures are easy to execute and conduct, and the equipment used in the experiments is cheap. On the contrary, results can change depending on the environmental variables, assessments may not detect the effects of the small changes, and assessments can't show the origin of the problem. System assessment tries to establish the source of the problem. The Balance Evaluation Test (BESTest) is the most widely used system assessment to identify the different balance disorders by investigating 36 items in 6 sections [6, 7].

Instrumental assessment is the other major examination method. It improves the rehabilitation process significantly by providing vital information about the working principles of postural control. Instrumental tests can examine static and dynamic balance. Quantitative posturography is an important member of instrumental measures that can supply detailed data by surpassing the significant weaknesses of functional examinations [8]. In short, it provides more consistent results and more sensitivity. Four main instruments are used to make the quantitative measure: force platforms, stereophotogrammetric devices, and wearable inertial sensors.

A force platform is popular equipment used in postural balance measurements. It detects vertical force applied to the platform's corners and generates a geometric center point called the center of pressure. According to the changes on COP, the experimenter can analyze the postural balance. Some platforms can also detect horizontal forces [9]. Spectrophotogrammetry is a unique type of photogrammetry. In that method, multiple photographic images are taken from different angles to provide 3D postural and movement information [10]. Wearable inertial sensors are another widely used instrument that measures a patient's balance or posture control. They are portable, implementable, and developable products of advanced technology. For example [11], researchers combined an accelerometer and gyroscope and built a system to measure body sway. Depending on the examination, the experimenter can use one or multiple instruments for more detailed diagnostics.

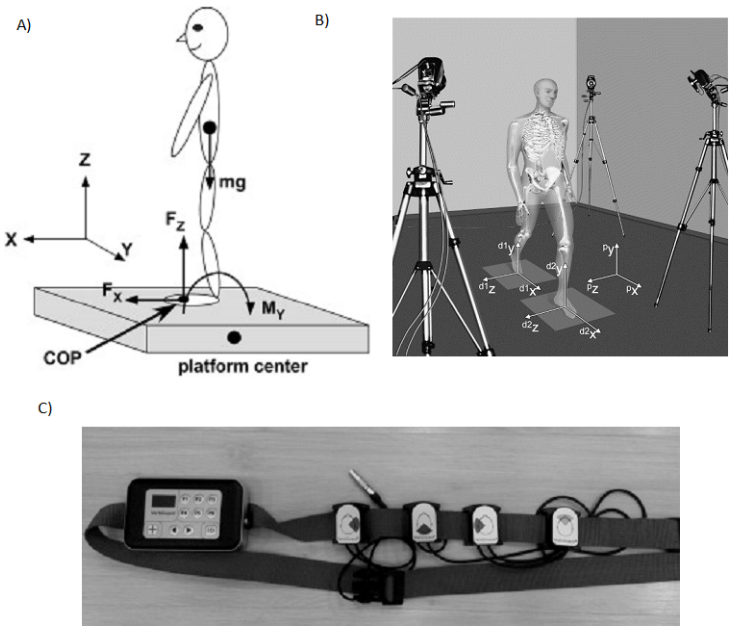

Figure 2.1 A) a representative force platform, "COP" shows the center of pressure, and "mg" shows the approximate location center of gravity. Fx represents the horizontal force, and Fy represents the vertical force. B) Stereophotogrammetry system to record the participant's gait from different positions to create a 3D model. C) Vertiguard wearable inertial sensors system that measures the body sway of the patient and provides vibrotactile feedback accordingly [12, 13].

Static posturography and dynamic posturography are significant and widely used instrumental assessments of postural control. In static posturography, patients try to stand still or in a specific condition on an instrumented platform such as a force platform, and their center of pressure changes are recorded. In dynamic posturogra-

phy, the only difference is external perturbations such as moveable platforms, visual contents, external sounds, and physical forces applied directly to the body (pull, push) are applied to the patient during the test [4]. Computerized dynamic posturography (CDP) is a quantitative method to measure posture control of the subjects under static or dynamic conditions. This posturography method provides three assessments: Sensory organization test, motor control test, and adaptation test. In the SOT, the experimenter applies visual and/or surface perturbation during the test and measures the balance performance while single or multiple sensory channels were disrupted. That will provide the performance of the remaining sensory channels. Six conditions are tested during the procedure, and those are shown in Figure 2.2.

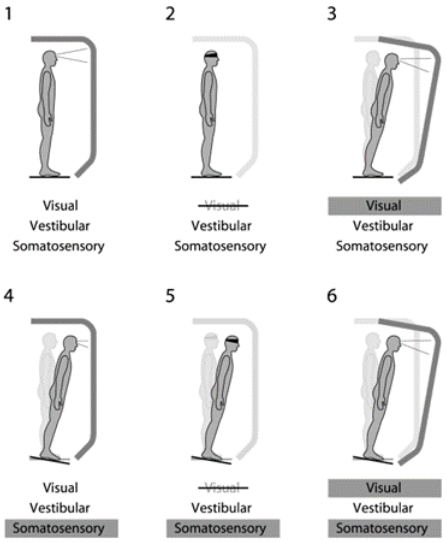

Figure 2.2 Six conditions of the SOT test [14].

This test provides an equilibrium score which represents the overall balance score by using the Eq. 2.1 12.5° is the maximum normal anterior-posterior sway, and θ is the center of gravity displacement of the participant. The result occurs between 0-100. A score of 0 means balance has been lost and a score of 100 means perfect stability [14].

$$x = \frac{12.5^\circ - (\theta max - \theta min)}{12.5^\circ} * 100 \tag{2.1}$$

After examination and diagnosis, treatment and rehabilitation processes begin. As balance disorders might depend on different diseases, their treatment and rehabilitation methods might also differ. For example, dopaminergic drugs and deep brain stimulations are used to improve balance functions [2], whereas exercises can reduce dizziness caused by the vestibular disorders. However, some shared balance improvement methods exist through wearable inertial sensors/circuits. Nowadays, many researchers use the vibrotactile feedback method to improve balance by providing vital posture information in real-time. Goebel et al. conducted a study to measure the effectiveness of vibrotactile feedback on patients who suffer from bilateral vestibular loss. They placed a headband with 4 C2 vibrating tactors on patients. Their body sway was recorded in real-time through Newton's Apple [1]. Another study is made by Marcos et al. to reduce falls in patients with Parkinson's Disease. They used the diagnostic tool of the Vertiguard to measure the body sway and four vibrotactile motors to give feedback about the body position of the patients [15]. Moreover, a similar study was conducted by Guiliana Ballardini et al. However, this time anterior posterior acceleration patterns of the participants were measured and tried to be reduced by using vibrotactile feedback. To achieve that, they placed a accelerometer to participants' approximate center of mass to record anterior posterior acceleration in real-time and depending on the current acceleration they applied stimuli in two vibrotactile strategy. First, they always keep the vibrotactile motors on and with the changing acceleration they increased or decreased the vibration frequency. In the second strategy, They kept vibration motors off until body acceleration reached to a certaion value then, they applied the stimuli and changed the frequency depending on the acceleration fluctuation [16].

2.2 Vestibular System and Posture

Humans invented devices like accelerometers and gyroscopes to measure the acceleration and rotation of objects many years ago. Nowadays, they reached a technological level that can provide almost impeccable measures. However, like many other vertebrates, the human body has already possessed that inertial guidance system known as the vestibular system for thousands of years. The vestibular system

includes five sensory organs in the inner ear, which supply linear and angular acceleration of the head. Acceleration of the head rotates hair bundles protruding from hair cells. That action impacts the membrane potential and causes synaptic transmission between hair cells and sensory neurons. Those sensory neurons transmit the captured data to vestibular nuclei in the brain stem. With that information, the eyes maintain their position while the head rotates. Also, preservation of the upright posture and awareness of own movement can be provided. Vestibular signals are generated in the inner ear through acceleration-sensitive organs in the membranous labyrinth surrounded by a hollow structure called the bone labyrinth. The bone labyrinth is located at the petrous portion of the temporal bone. Endolymph is a fluid with high Na+ and low K+ concentrations that fills the membranous labyrinth. In addition to this, perilymph is a fluid similar to cerebrospinal fluid. Opposite to the endolymph, it has high K+ and low Na+. A junctional complex prevents the fluids mixed up [17].

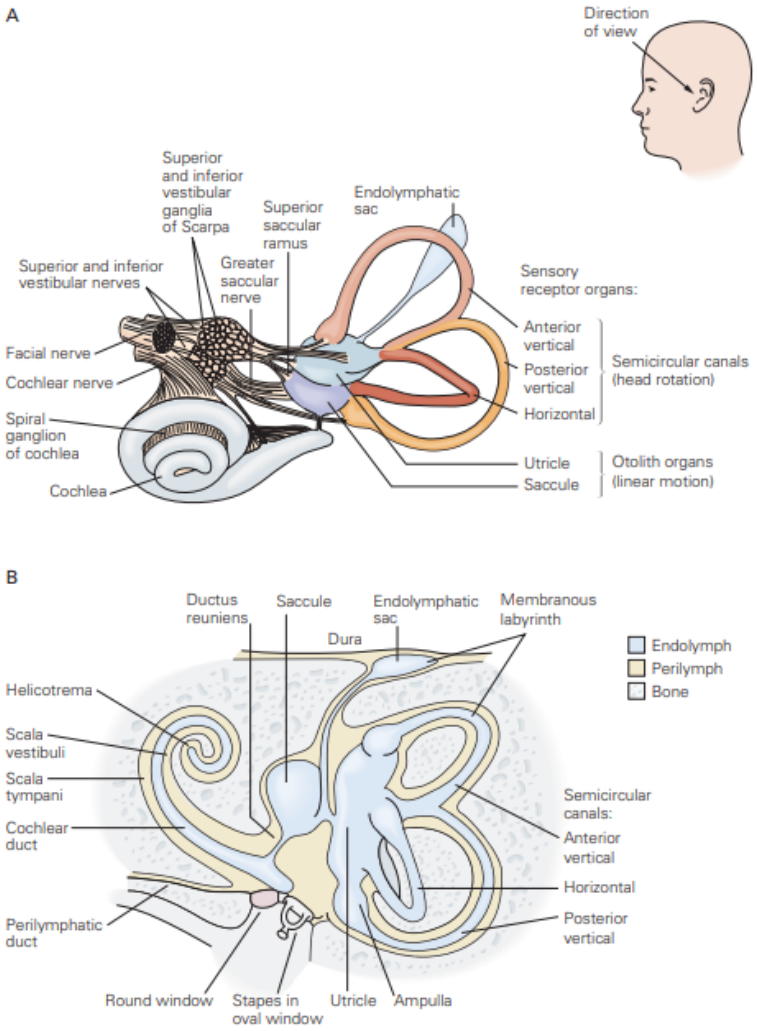

Figure 2.3 Inner layers of the vestibular system A) Coehlar and vestibular sections of the inner ear and its positioning depending on the head B)Bony and membranous labyrinths in the inner ear [17].

The vestibular apparatus is composed of three semicircular canals and two otolith organs. Semicircular canals (horizontal, anterior, and posterior) sense the rotation of the head. On the other hand, otolith organs (utricle and saccule) sense linear motion and head rotation against gravity because gravity is a linear force. All vestibular organs have one thing in common they possess hair cells to transform angular or linear acceleration into the vestibular signal. Specific acceleration stimulates the hair bundles in hair cells of specific organs by deflecting them. Then vestibulocochlear nerve (cranial nerve VIII) takes the signal to the brain stem. Vestibular ganglia of Scarpa have the cell bodies of vestibular nerve. Horizontal and anterior canals and utricle are innervated by the superior vestibular nerve. The posterior canal and sac-

cule are innervated through the inferior vestibular nerve. The vestibular system has multi-way communication with the brain stem. As it sends vestibular information, it receives efferent signals that affect the sensitivity of the afferent axons by changing the inhibitory postsynaptic potentials of the hair cells. When the body or head rotates through an axis, they undergo angular acceleration that deflects hair cells in semicircular canals. Then those canals measure the orientation and magnitude to report to the brain. Semicircular canals have two ends. The first of each opens to the utricle, and the other end opens to the ampulla. The gelatinous diaphragm, cupula, is located in the lumen of the canal. Cupula is connected to the epithelium along the perimeter, with hair bundles situated in it. The working principle of the vestibular orangs detecting acceleration is based on inertia. With the rotation of the head, labyrinths relocate with the head simultaneously, and endolymph stays behind the rotation of the membranous labyrinth and rotates within the canal in the opposite direction of the head movement. Endolymph passes through canals and stretches the cupula in the same direction as the flow. This flow causes a deflection on stereocilia of hair cells which leads change in membrane potential and firing rate of sensory fibers. This process is visualized in Figure 2.4 Semicircular canals are most sensitive to rotations in their planes, like the horizontal canal is most susceptible to the rotations in the horizontal plane [17].

Otolith organs, the utricle, and saccule are the part of the vestibular system which detects linear movement of the body and the orientation of the head germane to gravity. Both organs are comprised of a sac of the membranous labyrinth. Hair cells of otolith organs are located in a patch called macula. The otolithic membrane is a gelatinous structure that coats the macula, and hair bundles of the otolithic organ's hair cells extend into it. Millions of calcium carbonate particles are buried in the surface, known as otoconia. Linear accelerations like gravity apply a force on the otolithic membrane and otoconial matrix. This force can relocate the membranous labyrinth, which causes hair cells to be deflected. Depending on the deflection, the vestibular nerve can signal the features of linear acceleration to the brain stem. In some cases, these signals can be unidentifiable. So, the brain combines information from other vestibular organs (semicircular organs) and systems (visual and somatosensory) to assess motion. The working principle of saccule is similar to the utricle. However, the

saccular macula is oriented vertically to the para-sagittal plane, making it more sensitive to vertical linear accelerations like gravity. In the movement of the head rotation, semicircular canals of both ears work together. For example, while the head is turning, the horizontal canal on the turning side is excited while the canal on the opposite side is inhibited [17]. Vestibular and cochlear nerves form the vestibulocochlear nerve

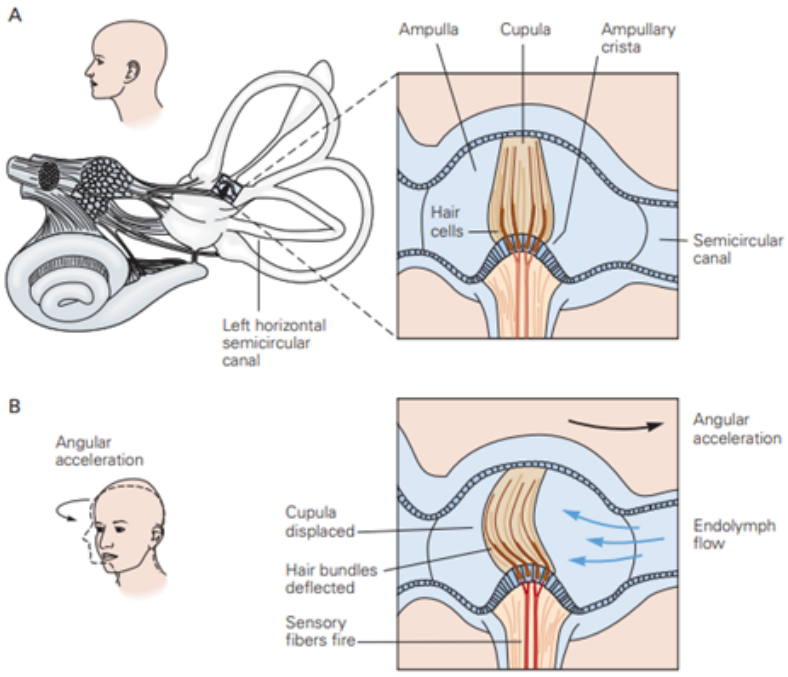

Figure 2.4 A) Zoomed field is the ampulla crista which contains the hair cells in it. The surrounding gelatinous diaphragm is called the cupula which connects the crista to the roof of the ampulla. B) Displacement of the cupula depending on the rotation of the head. Hair cells deflect the opposite direction of the rotation [17].

(cranial nerve VIII). The primary purpose of the vestibular nerve is to provide balance and eye reflexes [17, 18]. The vestibular neurons do synaptic transmission with both hair cells of both semicircular canals and otolith organs. Axons go through the internal auditory canal with cochlear division. The type of those neurons is bipolar, and their cell bodies are located in the petrous portion of the temporal bone. Cumulation of those cell bodies forms the vestibular ganglion, as shown in Figure 2.5.

After leaving the internal auditory canal, axons move through the lateral surface of the rostral medulla and enter the medulla between the caudal cerebellar peduncle and the spinal tract of the trigeminal nerve. Most nerves terminate in the vestibular

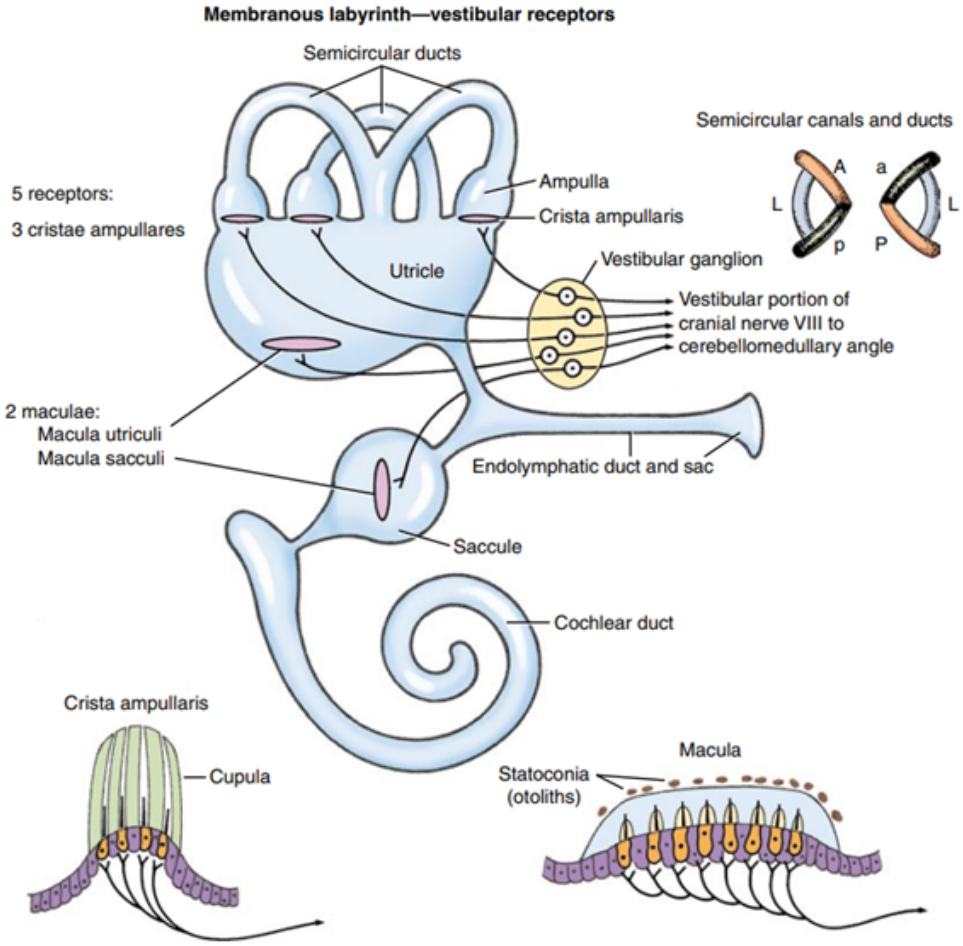

Figure 2.5 Vestibular system and part of it (membranous labyrinth and hair receptors in the ampulla and macula). On the top right side of the Figure, there is a representation of the Semicircular canals. A- anterior vertical, L- lateral-horizontal plane, P- posterior- vertical plane [17].

nuclei, which are located in the medulla and pons. Vestibular nuclei combine different signals collected from vestibular organs, cerebellum, spinal cord, and visual system and transmit them to central points like oculomotor nuclei, reticular, spinal centers, and each other. Four different nuclei (medial, lateral, superior, and descending) form the vestibular nuclei. Those nuclei have different cytoarchitecture and functions. Most fibers connected to the medial and superior nucleus come from the semicircular canals on both ears. Then they are transported to the oculomotor centers and spinal cord. The medial nucleus mainly possesses excitatory neurons opposite to the superior nucleus. Intended and steady looking is provided by those nuclei. On the other hand, the descending nucleus mostly takes information on otolithic organs and transmits it to several points: cerebellum, reticular formation, contralateral vestibular nuclei, and

spinal cord. The function of this nucleus is assumed to integrate the vestibular signal with the central motor signal and transmit that to the spinal cord. Finally, the lateral vestibular nucleus focuses on postural reflexes by receiving signals from semicircular canals and otolith organs and sending them to the lateral vestibulospinal tract [17].

Definition of posture is the current position of the body at a point depending on the alignment of joints [19]. Posture can be examined into two sub-groups, static and dynamic posture, depending on their stationarity. During static posture, body and aligned joints preserve their pre-configured positions. Lying, sitting, and standing still can be given as an example of static posture. On the other hand, in the dynamic posture, body parts do not remain stationary, and the body moves accordingly. Walking, running, jumping swimming are examples of dynamic posture [20]. While maintaining the posture, postural orientation and equilibrium need perpetual configuration according to the receiving data from several sensory systems. Postural equilibrium involves resistance to external and internal disturbances affecting the body [6, 17]. The most effective external force affecting the postural equilibrium is gravity. Posture orientation is the alignment of the joints relative to each other and the environment. Joints can realign depending on the ongoing tasks and environmental conditions [6]. Different animals possess different biomechanical features because of their unique anatomies and postural orientations. However, some species share similar postural control mechanisms, such as humans and quadrupedal mammals. The human is mechanically unstable without the guidance of the nervous system. The nervous system controls the position and motion of the center of the mass, a point that represents the average position of the total body mass, shown in Figure 2.6.

The center of mass does not have a specific location. It changes depending on the current posture orientation. Gravitational force affects the whole body, but the net effect occurs on the center of mass. Against the action of gravity, the surface reacts by the ground reaction force. The net ground reaction force forms on a presumptive point called the center of pressure. The base of support is an imaginary area formed by the body parts that contact the surface. While a person is standing without any help, the projection of the center of mass on the base of support should stay within the

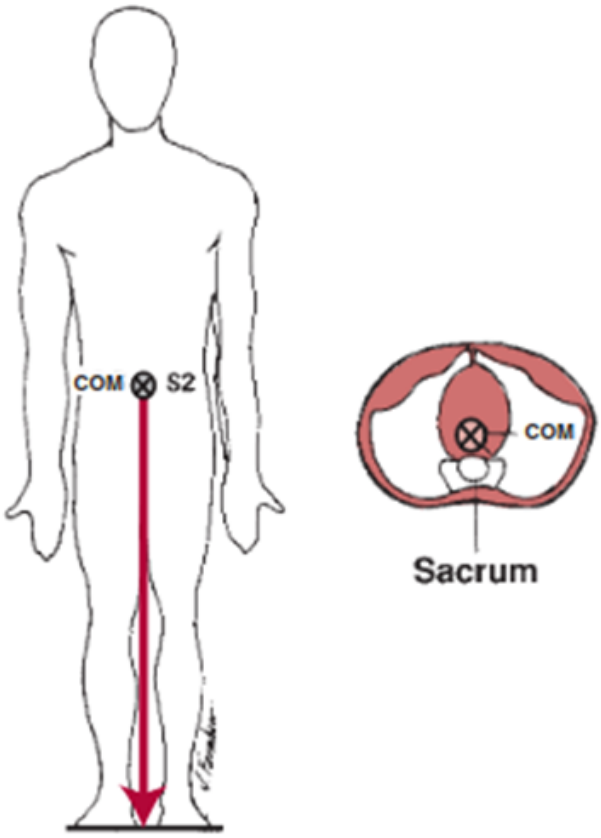

Figure 2.6 Center of mass of humans is approximately located around the S2 spin [20].

boundaries to maintain the balance. Also, In Figure 2.7, a cat stands on the ground on its four paws, and base support is shown between its four paws [17].

The upright stance is the default position of the body while standing still. Two conditions, resisting gravity and providing balance, must be fulfilled to achieve that. These conditions are controlled individually by the nervous system. To resist gravity, tonic activation of muscles creates a force that keeps the body parts extended and the center of mass above the ground. In the human body, bone-to-bone force in the joints is the main element that provides gravity support. In addition to that, active muscle contraction is also needed. Opposite to gravitational resistance, balance can't be maintained by only the tonic muscle activation [17].

A quiet stance is not a stable position. The human body always sways on the horizontal plane due to internal (breathing) and external factors. Actively contracting

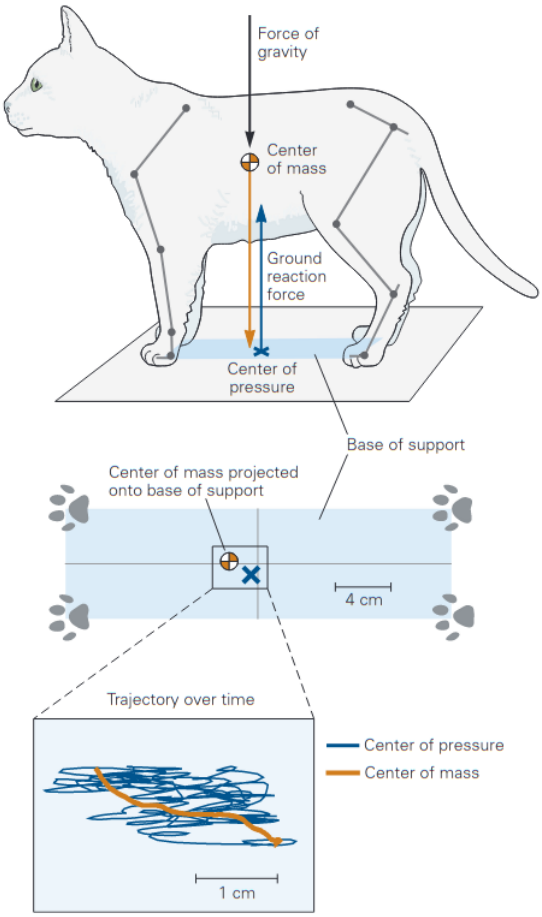

Figure 2.7 At the top of the Figure cat is standing on the ground. The Center of pressure and center of mass are both marked. The middle image focuses on the base of support and shows a closer image of the center of pressure also the projection of the center of mass on it. The bottom image zooms in the middle region of the base of support and shows the trajectory of both points over time. [17].

muscles partially reduce the sways' amplitude, but it is not enough to maintain the balance. Muscle activation in complex patterns is the most influential factor for muscle control by causing direction-specific force. Motor strategies are another important fact about balance control. There are two strategies commonly used in literature: ankle and hip strategy. As the name refers, in the ankle strategy after the disturbance, the base of support remains the same, and the person tries to regain his balance by rotating about his ankle. On the other hand, in the hip strategy, after the disturbance, the center of mass shifts to a direction, and the person either steps toward the direction of the shift or uses external support. An example of these strategies is shown in Figure 2.8. [17].

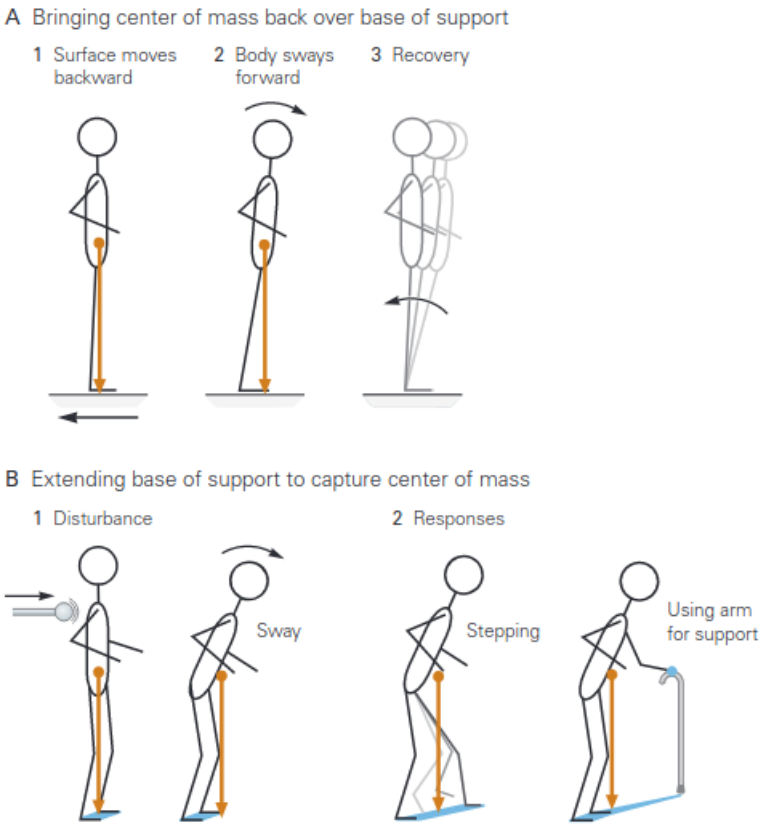

Figure 2.8 A) platform under the person shifts backward, but the integrity of the base of support remains. Avatar tries to regain his balance by rotating back about his ankle. B) An apparatus is used to provide external disturbance. The downward projection of the center of mass passes the boundaries of the base of support. In response, Avatar either steps beyond the new center of mass or uses external support [17].

Individual sensory systems might be insufficient when analyzing the posture. Because of that, signals recorded from multiple sensory systems are integrated into postural centers to provide different aspects of the posture. The somatosensory system provides vital information about the timing and direction of the automatic postural responses by using large-diameter fibers, which can rapidly transmit the signal. In any case, if those fibers become ineffective, the speed and amplitude of the sway of the center of mass increase. Thus, maintaining the balance turns into a more challenging process. Ia and Ib fibers are the largest fast transmitting afferents. Ia fibers receive signals from muscle spindles, while Ib fibers receive theirs from the Golgi tendon organ and cutaneous mechanoreceptors. Fibers in group I are crucial to procure biomechanical information like muscle stretch, muscle force, and the direction of the force on the sole. Fibers part of group II might also be useful for automatic postural responses.

However, they might be slow to generate an early response. Postural orientation is a complex task, and many modalities of the sensory system have an essential part to play. For example, under the force of gravity, proprioceptive receptors detect information about features like the load that occurs on the muscle, muscle length, stretch velocity, or applied pressure on joints can be spotted by the joint receptors. Moreover, cutaneous receptors in the sole are responsible for detecting the changes in the center of pressure. The vestibular system provides balance information through semicircular canals and otolith organs. Otolith organs detect linear acceleration, including gravity, and semicircular canals detect the angular acceleration of the head. Finally, the visual system provides great balance support for voluntary actions. Such as planning to climb a tree or go through over an obstacle [17].

Processing postural information and providing balance and orientation is conducted from the spinal cord to the cerebral cortex. The spinal cord can manage the antigravity support, but balance control needs supraspinal circuits to do the task. The exact supraspinal centers that control automatic postural response are unknown. However, the cerebellum and brain have an interconnected structure and work together to modulate motor signals. Because of that, they are considered to be the centers of postural control. The brain stem is thought to control the muscle synergies, while the cerebellum controls the postural adaptation. Two regions in the cerebellum affect the balance and orientation: vestibulocerebellum and spinocerebellum. They communicate with vestibular nuclei and reticular formation of pons and medulla. Vestibulocerebellum damage can cause a reduction in head and trunk control and increase vertical tilt even when eyes open. On the other side, Spinocerebellum injuries can cause excessive postural sway, especially when the eyes close. Specific areas in the medulla and pons can be effective on gravity support by facilitating and depressing the extensor tonus [17].

2.3 Somatosensory Feedback

The somatosensory is one of the primary senses that includes five modalities: touch, proprioception, pain, itch, and visceral. The somatosensory system has three main functions. These are proprioception, exteroception, and interoception. Proprioception is the sense of oneself. Receptors in the skin, joint capsules, and skeletal muscles provide posture and movement awareness information. Lack of proprioception will cause adverse effects on movement, coordination, and ability to do complex tasks, especially if there is no visual information. Sense caused by direct contact with the environment is known as Exteroception, which includes touch, pain, and thermal senses. The sense of touch has multiple sub-modalities: contact, stroking, pressure, motion, and vibration. Thermal sense involves sensations of heat and cold. Finally, interoception is the sense of organ systems. It is essential to get information about organ functions through chemoreceptors and organize them [17].

The sensation process starts at the dorsal root gangion's receptor terminal. Specific stimuli activate unique receptors on joints, muscles, skin, or internal organs. For example, chemical changes in the body are detected by chemoreceptors, or heat change in the environment will activate the thermoreceptors on the skin. Somatosensory, auditory and vestibular systems use mechanoreceptors to detect multiple modalities: touch, hearing, proprioception, and head motion. After receptors detect sensory information, dorsal root ganglion neurons encode the signal and transmit it to the central nervous system(CNS). This process is shown in Figure 2.9 [17].

Mechanoreceptors are a unique type of receptor which is activated via physical deformation. Mechanical stimuli on the skin deform the protein of mechanoreceptors, opening the stretch-sensitive ion channels and increasing the conductance of Na+ and Ca+2 to move into the receptor neuron and start depolarization. If the stimulus is strong enough, it makes sensory neurons fire an action potential that travels from the peripheral branch to the central branch and stops at the spinal cord or brain stem. Cutaneous and sub-cutaneous mechanoreceptors are responsible for the sensation of touch. Those mechanoreceptors have eight unique members located in some parts of

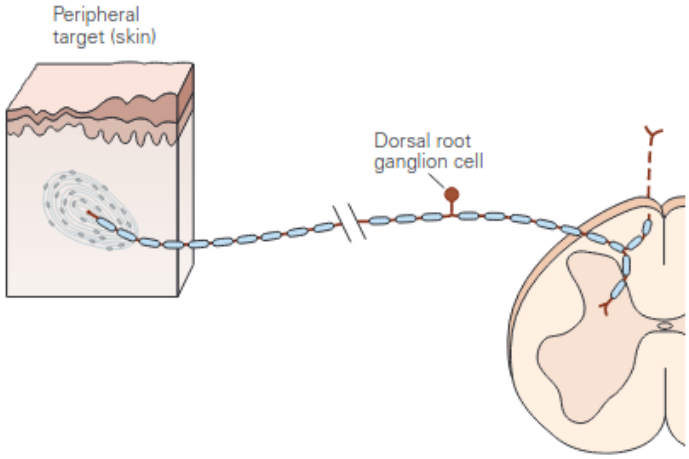

Figure 2.9 1 Neuron has two axon branches. The first branch receives the signal from the receptor terminal, and the second branch transmits the signal to the segments of the CNS. The cell body of the neuron lies in the dorsal ganglia [17].

the skin. Glabrous and hairy skin share some common mechanoreceptors. However, they possess some unique mechanoreceptors as well [17].

Firstly, glabrous skin contains four different mechanoreceptors. Those mechanoreceptors differ according to their morphology, innervation patterns, and location in the skin. As innervation, they are divided into two groups depending on the axon's adaptation skill they connected: rapidly adapting and slowly adapting. Rapidly adapting fibers react to the changes in the stimulus, while slowly adapting fibers respond to the sustained stationary stimuli. Tactile sensation in hand is provided by four different functional units(SA1, SA2, RA1, RA2) formed by an adaptive fiber, a receptor connected to the axon terminal, and the fiber's distal branch [17].

SA1 fibers are spread across the skin, particularly on the fingertips. In the receptor terminal, they use the Merkel cells as receptor organs. Merkel Cells are specialized epidermal cells that surround the unmyelinated terminal of the SA1 axons. The connection between the Merkel cells and axons occurs through synapse-like junctions. Merkel cells react to momentarily or consistent pressure and best provide information about edges, corners, and pointy surfaces. They are located close to the skin surface. Ruffini ending is a low-threshold slowly adapting mechanoreceptor [21]. Ruffini end-

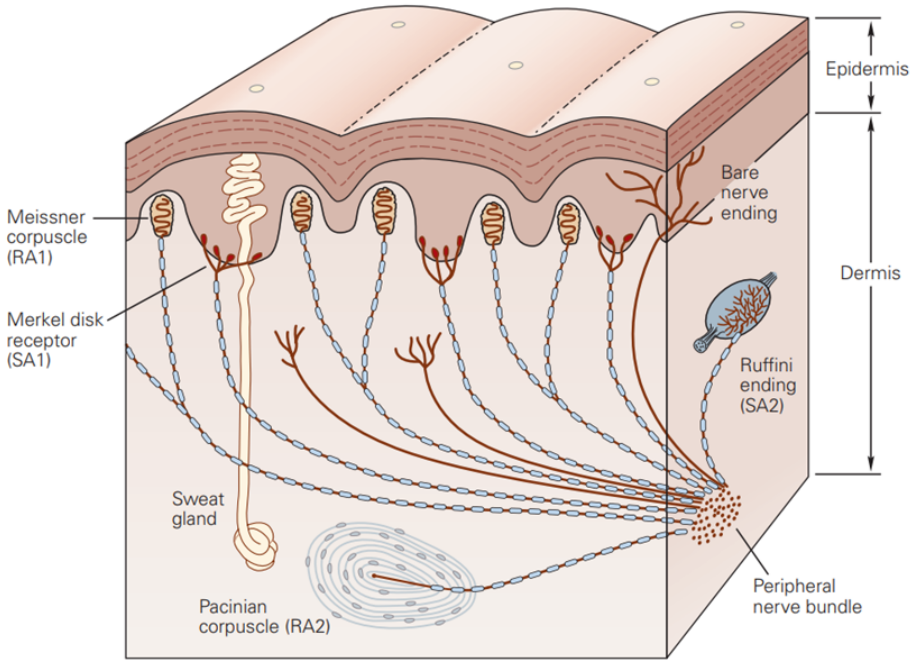

Figure 2.10 A section taken from a glabrous skin that includes both dermis and epidermis and mechanoreceptor [17].

ings lay at the receptor terminal of the SA2 fibers. They are sensitive to skin stretch. Meissner corpuscles are rapidly adapting mechanoreceptors located in the superficial bumps of the dermis (Figure. 2.10). These mechanoreceptors respond to low-frequency skin motions like running a finger over an object (roughness and smoothness will also affect the mechanoreceptor response). They are positioned at the terminal end of the RA1 fibers. The final mechanoreceptor in the glabrous skin is the Pacinian corpuscle. These mechanoreceptors are located in the depths of the dermis with an onion-like capsule [17, 22]. Because of that, they have a large receptive field. They are sensitive to high-frequency vibrations. They are attached to the terminal end of the RA2 fibers.

Hairy skin covers most of the body surface. In contrast with glabrous skin, it has hair follicles rather than Meissner corpuscle for the same function. Hair follicles can position from the epidermis's surface to the dermis's depth [17, 23]. In addition to those mechanoreceptors, hairy skin possesses field receptors and C, hair-guard, hair-up, and hair down mechanoreceptors.

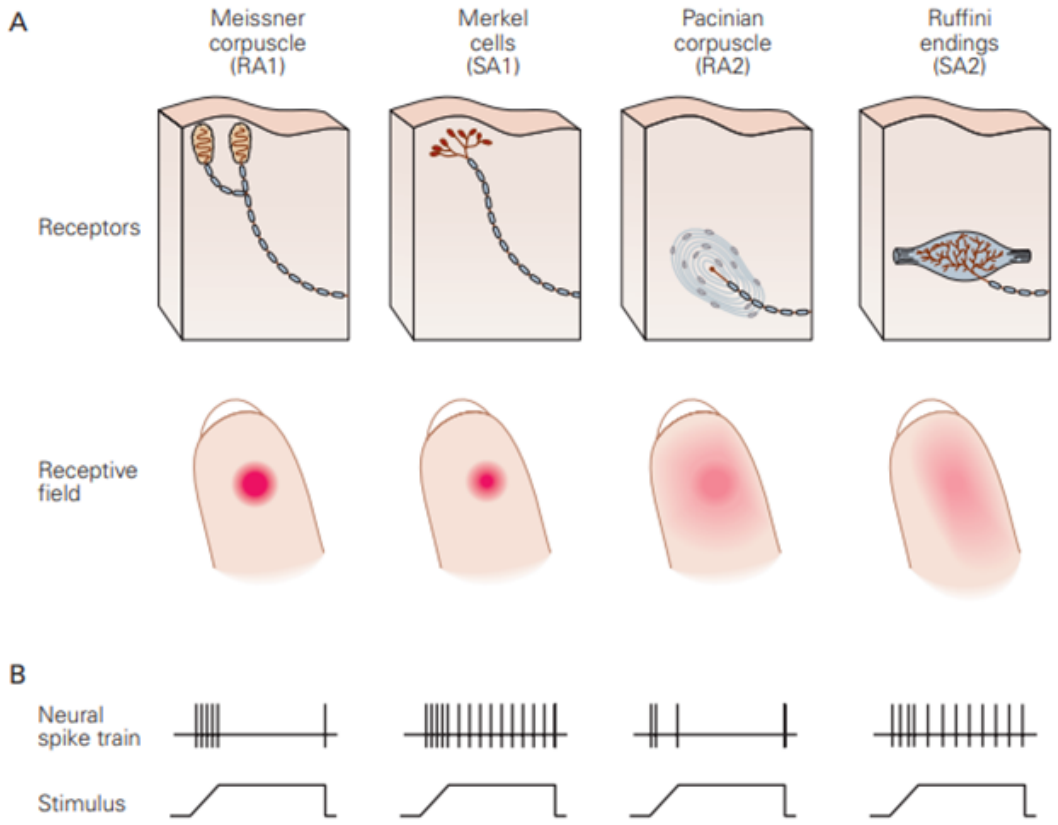

Figure 2.11 Mechanoreceptors in the glabrous skin. Receptors located near the surface have smaller receptive fields. Also, encapsulation is another factor in the size of the receptive field. B) Slowly adapting fibers respond frequently until stimulation is over. However, rapidly adapting fibers only respond to changes in the stimuli [17].

Psychophysical channels prosess information from sensory inputs. There are four channels assotiated with glabrous skin mechanoreceptors: The Pacinian channel (P) and Non-Pacinian (NPI-NPII-NPIII). They play a significant part in perception by processing the tactile information and integrating the result within the Central Nervous System. The Pacinian channel is mediated by the Pacinian corpuscles. Its effective frequency range is 40-800 Hz. In that range, it has a U-shape tuning curve, and according to Verillo et al., it is most sensitive to frequencies around 300 Hz [24]. Moreover, this channel type is quite sensitive to temperature [25]. It reacts to dynamic stimulus size and duration. Pacinian channel can do the spatial and temporal summation. Due to spatial summation, increasing the stimulation area will decrease the threshold. Due to the temporal summation effect, the detection threshold will decrease if the stimulus duration increases [26–28]. NPI is mediated through the Meissner cor-

puscle; Its effective frequency range is between 10-100 Hz [29–31]. NPI channel is not affected by temperature or changes in stimulus frequency [26, 32–34]. Ruffini endings mediate the NPII channel. Its effective signal range is similar to the P channel but has a smaller receptive field. Finally, the NPIII is mediated through Merkel cells. It can operate between 0.4 and 100 Hz. Figure 2.12 shows the thresholds of the four-channel depending on the stimulus frequency and amplitude. The frequency ranges mentioned above reffered the sensation at threshold.

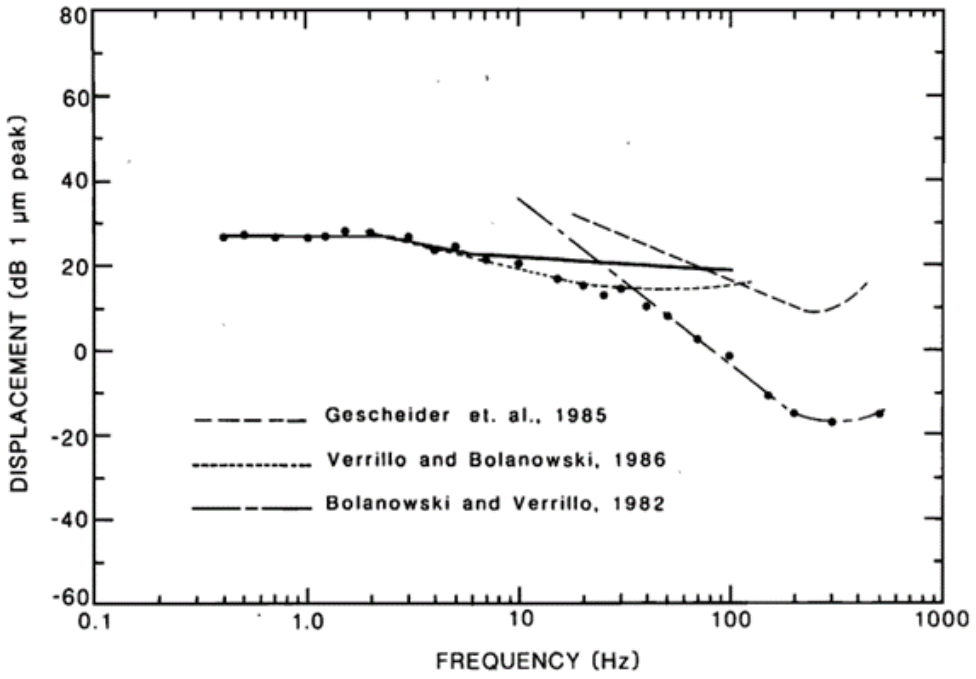

Figure 2.12 Displacementthreshold values of the four mechanoreceptive channels. -.-: PC, - - -: NPI, ___: NPII,___: NPIII [35].

Hairy skin sensitivity also changes with the contactor size. Also, its vibrotactile thresholds are higher than glabrous skins. Fig 2.13 shows the threshold difference between glabrous and hairy skin.

There is a quantitative relationship between stimuli and sensation. Psychophysics is a scientific method that investigates that relationship. Any member of the sensory systems can be examined through psychophysical methods. To conduct a psychophysical experiment, five principal components must be obtained: stimulus, task, method, analysis, and measure. The stimulus is the component used to activate the selected

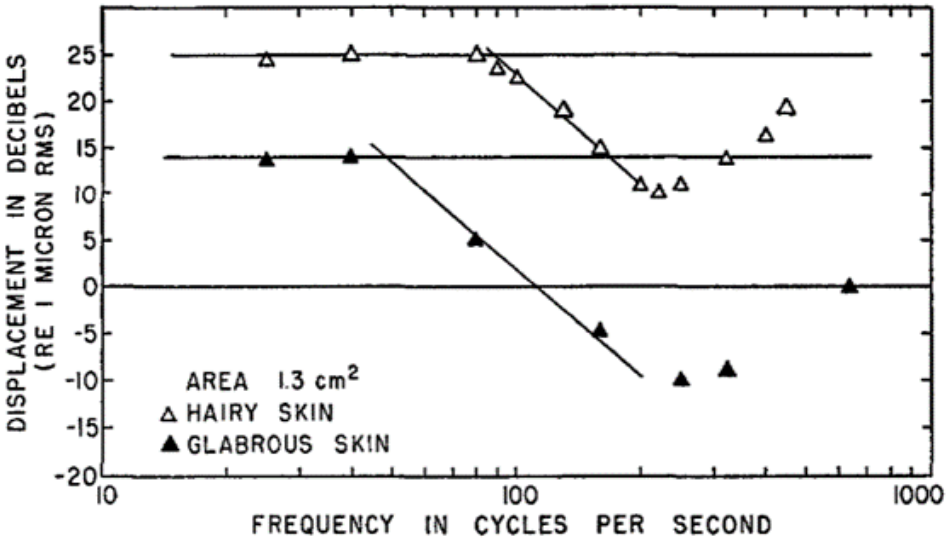

Figure 2.13 Threshold comparison depending on the frequency and amplitude between the hairy and glabrous skin [36].

sensory system. It is the least generalizable component. The task is the action that the participant must do for each trial. The method is how the stimulus is applied and how the experimenter observes the participant. In the analysis part, the experimenter processes the row data to a meaningful output. The measure is the outcome according to the analysis. One of the first experiments designed to measure the weakest detectable stimuli is absolute threshold detection. The other one designed to calculate the discrimination threshold is the difference threshold, also known as Just noticeable difference [35].

Those measures are essential to calibrate somatosensory feedback. Somatosensory feedback is used to provide information about specific conditions by stimulating the somatosensory receptors. For example, Karakuş and Güçlü used vibrotactile feedback to supply the position and motion status of the neuroprosthetic [37]. Somatosensory feedback can be applied in invasive or non-invasive ways. Invasive procedures require surgical operations to implant the stimulator inside the body, and the stimulation type is the electrical stimulus directly applied to the peripheral or central neurons. On the other hand, non-invasive stimulation doesn't require any surgery, and stimulation is applied to the skin surface. Also, the stimulation type might be electrotactile, vibrotactile, or mechanotactile [38]. Electrotactile feedback is provided by applying a small

current to the skin to evoke the afferents [39]. Different from electrotactile feedback, vibrotactile feedback is generated by mechanical vibrations. In vibrotactile feedbacks, duration, frequency, and amplitude are adjustable parameters. In most applications, the preferred vibration frequency range is between 10 Hz to 500 Hz. Mechanotactile feedback is provided by applying pressure to specific area of the surface depending on the encoded message.

2.4 Virtual Reality and Augmented Reality

Virtual reality (VR) systems present an interactive three-dimensional environment in that users can experience visual, auditory, and tactile elements through several devices like headphones, head-mounted screens, and haptic feedback equipment. Some systems also use motion capture tools to track and transmit the motion of the user to the system. Mostly, those devices isolate the user from the real world by eliminating the coming stimuli [40]. Quality of the VR products is increasing with developing technology. The origin of VR dates back to the 1960s; a computer scientist named Ivan Sutherland published a paper, "The Ultimate Display" and designed the first head-mounted display (HMD) with a head tracking system in the next three years. That was a revolutionary invention for VR technologies [41]. Even today, companies use similar equipment based on Sutherland's design. For example, an American company named Oculus designed an improved version of the HMD (Figure 2.14) in visual, auditory, and navigational aspects.

For visual improvements, they used a high-definition OLED screen to achieve high graphic quality. Along with it, well-placed adjustable lenses provide a wider perspective. For auditory improvements, they placed a speaker that can generate 3D environment sounds. And for navigation improvement, they placed an integrated circuit with a gyroscope and accelerometer that can measure the rotation and acceleration of the user's head [42]. However, using only two types of sensory feedback can be insufficient to create a realistic experience. Thus, combining the haptic interface with previous equipment might increase the perception level by activating the somatosensory

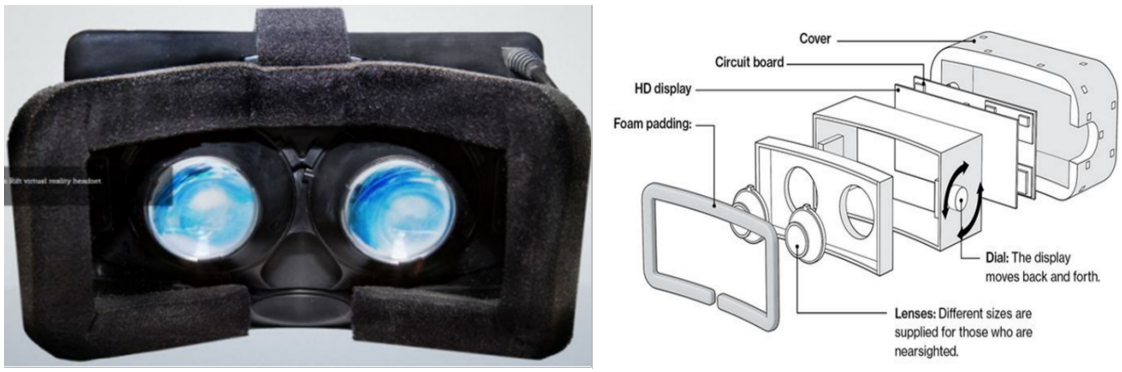

Figure 2.14 Left side of the Figure is the external view of an oculus rift, and the right side shows the device's internal layers [42].

system.

Haptic interfaces use touch and kinesthesia to create a communication line between people and machines. Arduino provides flexible, low-cost, and practical solutions to design a haptic interface. In that study, we used a particular model, Arduino Uno, to provide haptic feedback. Arduino UNO is an Atmega 328-based microcontroller card. It has 14 digital input/output and 6 analog input pins. Also, it has a USB port that provides communication between compatible computers [43]. In addition, Arduino can integrate with several communication tools such as Bluetooth and Wi-Fi modulators to provide wireless communication. Arduino has its programming language called Arduino programming language (APL). This programming language is based on C and C++. Arduino apps are written on an easy-to-use free IDE (Integrated Development Environment) platform. After the programming, the AVR tools package converts computer codes into microcontroller instructions [44].

Choice of hardware is crucial for VR systems. However, it is just as important on the software and modeling side. To establish an intense VR experience, the virtual environment and assets in it must be detailed and realistic. To provide that, we used Blender software. Blender is an open-source 3D object and animation program that uses engineering transformation to provide high-quality texture, shading, lighting, and rendering [46]. Also, it is compatible with many powerful programs like Unity3D or Unreal Engine and programming languages like python, C++, and C. To design

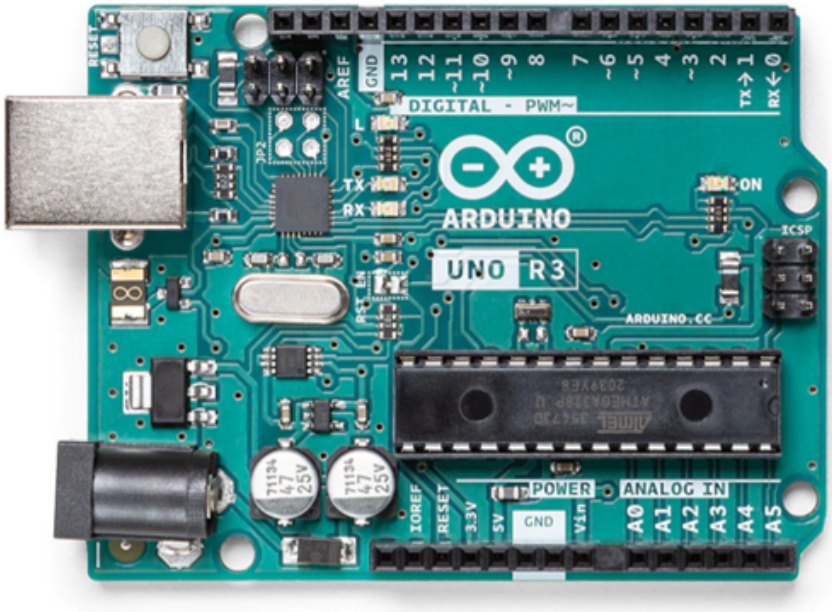

Figure 2.15 A new model Arduino UNO. 14 pins on the upper side of the board (0-13) are digital input/output pins and six pins on the lower side are analog input pins (A0-A5) [45].

the simulation, we used Unity 3D program. Unity3D is intended as a game development tool by Unity Technologies. However, its implementation area became wider. Through Unity3D, 2D/3D video games and simulations, visualization of structures and equipment, and real-time 3D animations can be created. Moreover, the programmability of Unity3D provides a dynamic and adjustable environment. It mostly uses the C programming language, but it can also run scripts of some other languages such as python and C++ by additional plug-ins [47]. Unit3D can also communicate with other programs and devices in real-time. For example, in our study, we developed an Arduino-based vibrotactile feedback design connected to Unity3D. Arduino was producing vibrotactile stimuli depending on the running simulation in Unity3D.

Virtual reality is an expanding market spreading to multiple fields such as medical, military, entertainment, and applied and theoretical science [48]. For example, Yi Wang et al. developed a procedure to train astronauts in space missions. They created a virtual environment through Unity3D and for guidance they designed a vibrotactile stimulation system. At the end of the experiment, results show that participants who learned the experiment procedure and completed the task through virtual reality had

a higher success rate. Medical applications of virtual reality are quite promising and significant. Because in contrast to high-tech hardware-based procedures, virtual reality can provide safe and low-cost methods to proceed. Recent studies show that it can be used for mental and physical therapies. For example, Chih-Hung Chen et al. designed a virtual-reality-based physical rehabilitation therapy for patients with low spinal cord injury. According to the results, patients running the task in VR were more relaxed and calmer than people in the control group [49]

Augmented Reality (AR) is another promising approach to building an informative virtual environment. Unlike Virtual Reality, Augmented Reality does not isolate the user. It interacts with the real world by mostly adding superimposed images to the participant's view. AR can be supplied via several devices like VR. The most common way to provide AR is using a cell phone camera. Today, through several applications, any smartphone can superimpose the real image with a virtual image. For example, a mobile application called ARLOOPA can add real-size dinosaur animations into the camera view. However, there are also more advanced and effective devices that are produced for a better AR experience as well. Same as VR, AR can be provided through head-mounted displays. Although, their design is different than VR headsets. For example, in the Microsoft Hololens headset, transparent lens, lighting, mirrors, and image processors are used to mix the real image with the virtual one [50]. Red, green, and blue lasers generate photons transiently. Then those photons travel through mirrors and scanners to create the virtual image. Finally, the image is projected to the special lenses. Figure 2.16 shows the pathway of the photons. AR devices can also provide auditory and haptic feedback in the same way as VR devices.

Well-designed and calibrated AR systems can supply useful information about the environment and objects to the user. Also, it makes creating a virtual simulation ground in the real world possible. Because of that, AR technology is getting more popular in several fields. For example, in medicine, invasive surgical procedures require precise visualization. Thus, surgeons use special scans before and during the operation for guidance, such as fluoroscopy and computed tomography. However, continuous usage of those methods causes radiation exposure for the doctor and the patient. There-

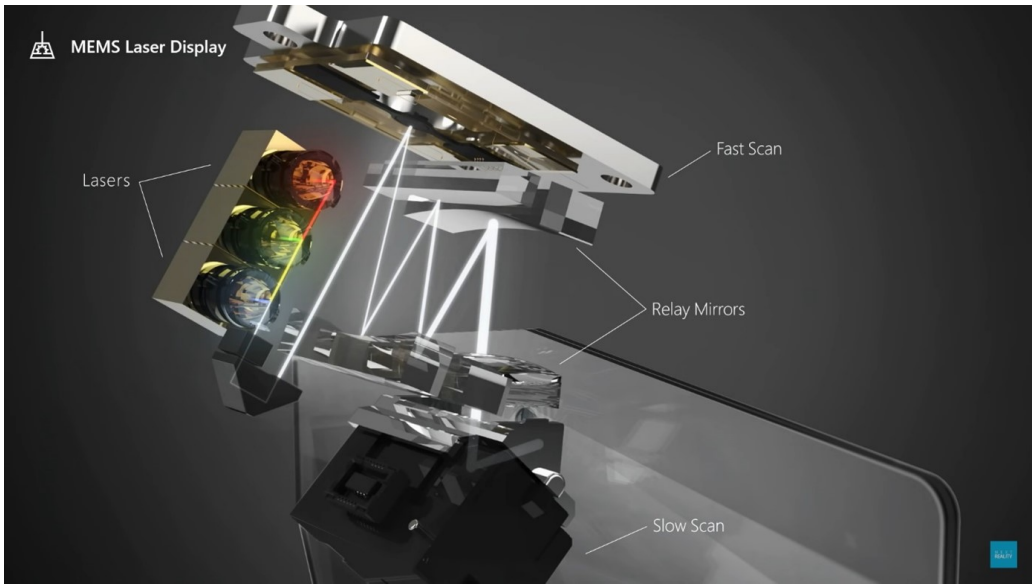

Figure 2.16 Creation of the virtual image in Microsoft Hololens 2 [51].

fore, Jacob T. Gibby et al. developed a real-time visual guidance procedure for pedicle screw placement by using augmented reality. They aimed to record the CT image once and train the system according to that image. Thus, the trained system could show the 3D CT image of the lumbar vertebrae on the back of the patient. To try that procedure, they used silicone to print a 3D block that represents the L2-L3 vertebrae. Then they trained the HMD with a real CT image of L2-L3 vertebrae. That way, HMD could project the CT image of the real vertebrae on the 3D silicone block. After they provided the projection, they tried to place the 36 needles into the pedicle part of the vertebrae. As a result, they placed 35 needles into the pedicle only 1 needle remained outside of the region [50].

3. MATERIALS AND METHODS

3.1 Experimental Setup

Only one participant attended the experiments. The experiments were approved by the Institutional Review Board for Research with Human Subjects of Bogazici University. Visual content is provided on a laptop screen 60 cm away from the head level of the participant. Feedback is controlled by the Arduino UNO microcontroller connected to a computer (DELL G3), and the communication port establishes communication between them. Six identical VIBRATION ERM MOTORs 3V (Seeed Technology Co., Ltd, Manufacturer Product Number: 316040001) are located on an armband in predetermined order was used to apply the vibrotactile feedback. White noise is given to the participant through headphones to eliminate the environmental noises. The experimental setup is presented in Figure 3.1. Visual contents were designed in the Blender and Unity 3D programs. Vibrotactile feedback is generated through Arduino Uno and provided to the participant by vibration motors. The participant completed the visual and the parkour experiments by pressing the arrow key that leads to sway direction. Vibrotactile stimuli were not used in visual experiments, and visual elements were not used in vibrotactile experiments.

First visual psychophysical experiments, then vibrotactile motor localization and avatar identification experiments were completed. Pooled data were used to configure the parkour experiments.

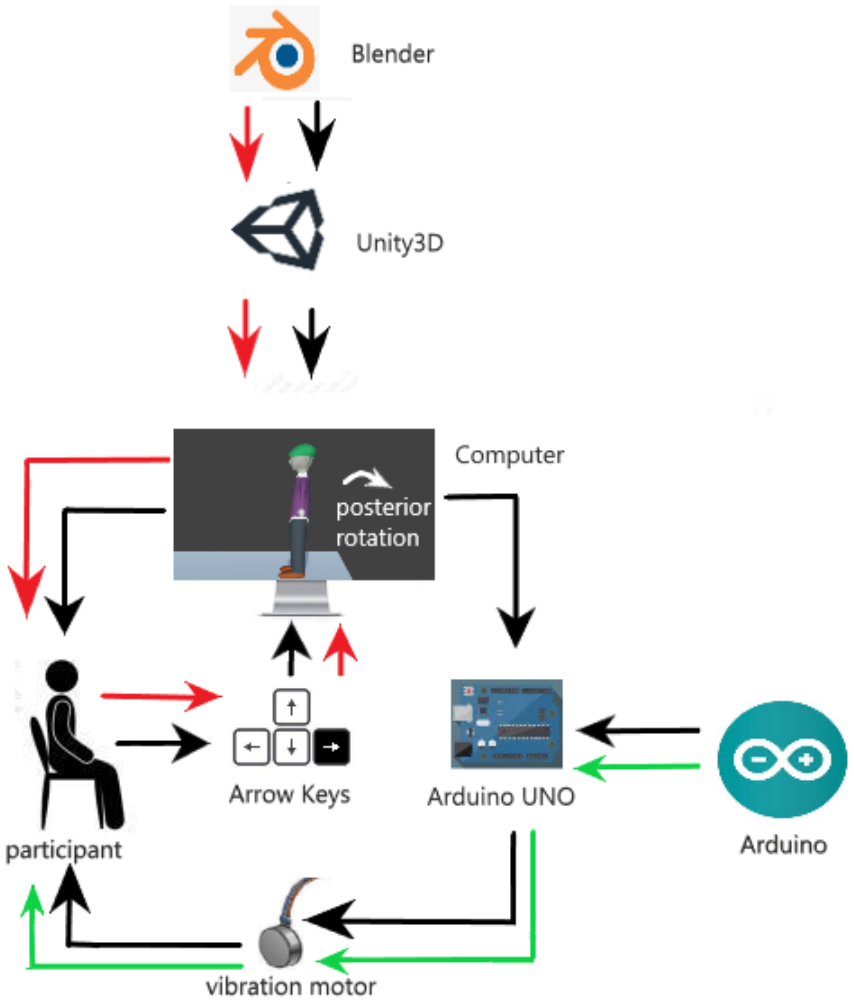

Figure 3.1 Diagram of experimental Setup. Red arrows shows the interaction path of the visual experiments, green arrows shows the interaction path of vibrotactile experiments and the black arrows shows the interactive path of the parkour experiment.

3.2 Modeling and Simulation

In this study, four experiments (Motion detection, angle discrimination, velocity discrimination, the parkour experiment) were based on visual contents. Instead of using premade assets, we designed our objects and avatar. Blender v3.1 were used to create our virtual 3D objects (Avatar, ground, cue) that are shown in Figure 3.2. Avatar was the focal point of the visual experiments. The participant had to follow its moves to complete their tasks. Its design is based on a middle-aged white male person with colorful clothes (Figure 3.2). We tried to make his appearance as noticeable as possible and his coating as soft as possible. So the participants could follow the the avatar,

did not spot the motion due to unnatural sharp and pointy edges. After the modeling, those objects were extracted as asset packages and implemented to simulations made in UNITY.

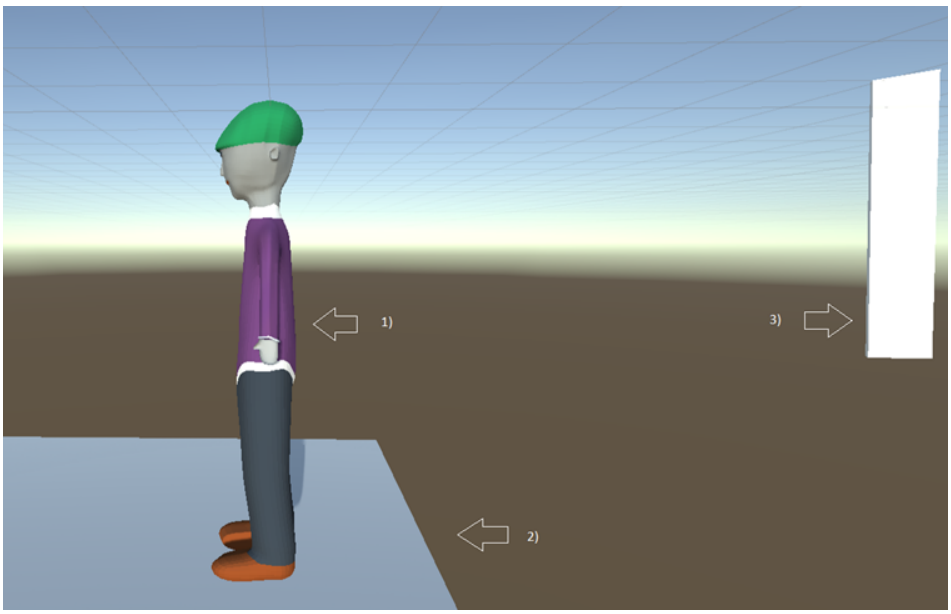

Figure 3.2 Image from the last experiment 1) Avatar, the main character of the visual experiments 2) Proving ground, 360 m open pathway without any obstacles.3) Cue, an object which shows the condition of the avatars' body sway by color codes .

Four simulations were designed in total, three for psychophysical experiments (Motion detecion, angle discrimination, and velocity discrimination) and one for the parkour experiment. For experiments involving motion, (motion detection, velocity discrimination and the parkour) I added smooth and aesthetic animations (walking, anterior/posterior body sway about avatar's ankle) to simulations at 90 fps. The participant gave his responses in real-time by using a keyboard. Answers were collected also through the UNITY3D. At the end of the every session, answers were extracted from the UNITY to an excel sheet. No biomechanical and physical laws were applied in the simulation. However, the avatar was programmed to sway with constant angular velocity to a pre-defined position according to the experiments.

3.3 Vibrotactile Feedback

Vibrotactile feedback was used to encode the avatar's rotation velocity and rotation angle. Electrical signals were generated through Arduino UNO and converted into vibration through six eccentric rotating mass motors (VIBRATION ERM MOTORs) shown in Figure 3.3.

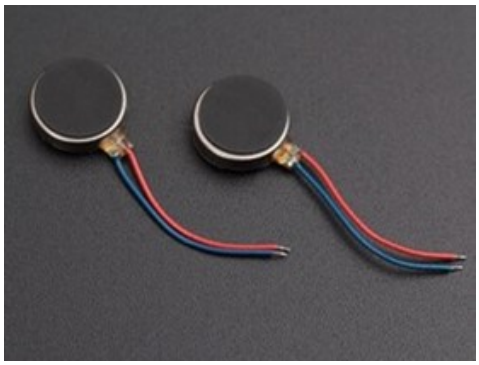

Figure 3.3 Vibration motor (Vibration ERM motor 3V / Seeed Studio) [52].

Those motors were divided into two groups to represent the anterior and posterior rotations. Motors in the anterior group were named Anterior Rotation Encoding Motor (AREM1-3), and in the posterior group are named Posterior Rotation Encoding Motor (PREM1-3). Motors were placed on an armband in a unique position and the armband were fixed on a circumferential line at the upper arm, one-third the length of the upper arm above the elbow. According to Matthieu Guemann et al., that is the most sensitive spot that can be stimulated without invoking the joint receptors. AREM1 was placed on the middle of the biceps, and others were placed medially. On the other hand, PREM1 was placed in the middle of the triceps, and others were located laterally. Distance between motors was one-twelve of the width of the placement site.

ERM motors are DC-type motors. The effective range of the motors is between 2.5 V and 3.5V. While generating the vibrotactile stimuli, we can't configure amplitude and frequency separately for this motor type. Thus, we fixed stimulus to 3.3V to produce vibration with fixed frequency and amplitude which causes no noxious feeling but is easy to detect. Also, it was generable by Arduino UNO without any extra

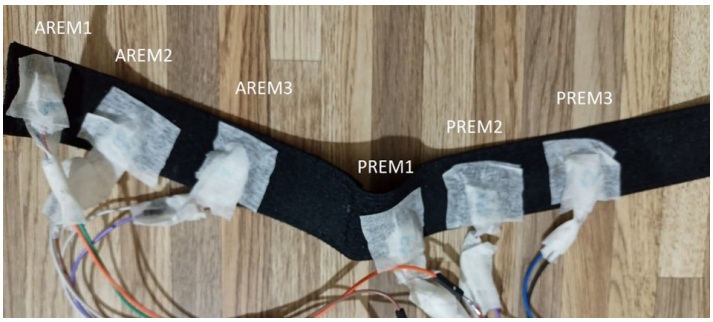

Figure 3.4 Installed armband.

adjustment. Then, we manipulated the vibration to produce mixed and pulse-number modulation to encode the sway velocity. In mixed modulation we generated two stimuli by changing the pulse width and pulse-numbers. First stimulus was formed by single pulse with 1s width and second was two pulse with 475ms width and interval between them was 50ms. Then, only pulse-number modulated stimuli were produced by using 50ms unit vibration. Stimuli were presented in Figure 3.5. Also, the amplitude were controled by recruiting additional motors incrementally, which causes a broader area to be stimulated and more mechanoreceptors to be evoked.

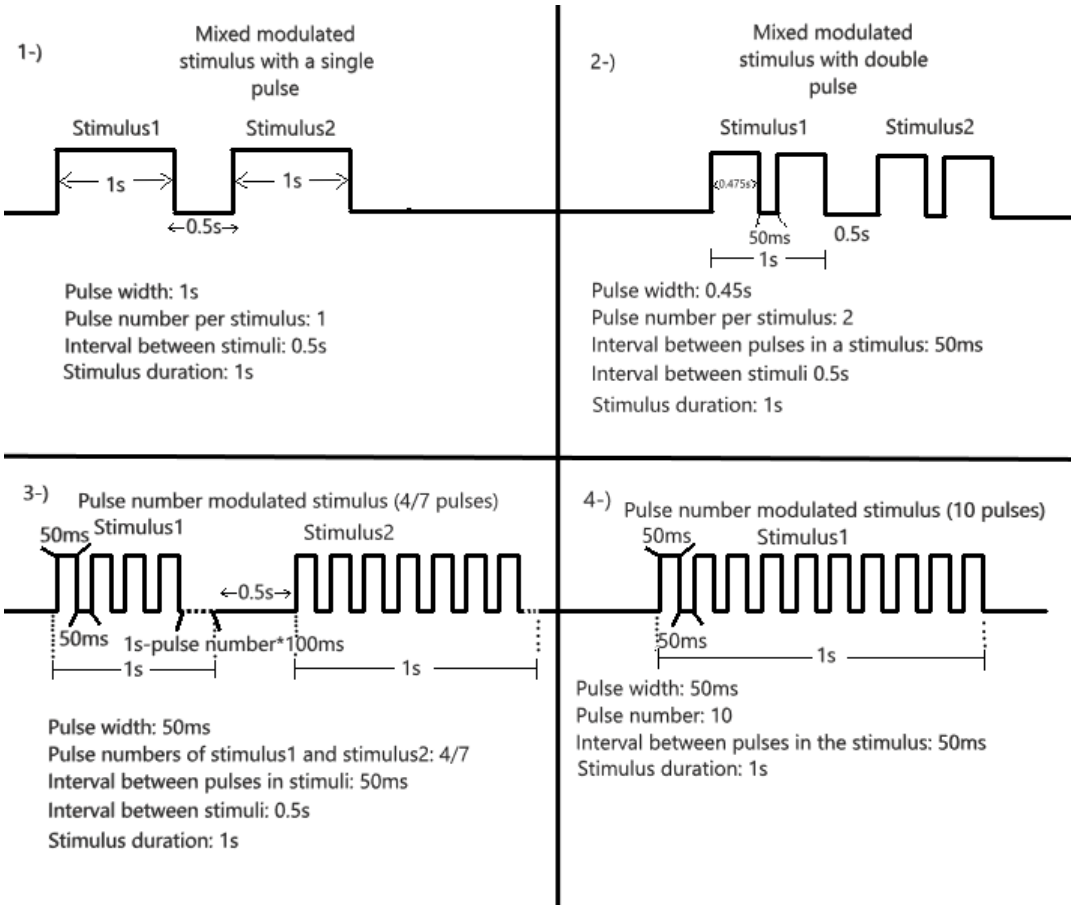

Figure 3.5 Actuation signals for vibrotactile motors designed to use in the parkour experiment. The actual vibrotactile stimuli are mechanical during the on periods shown in the panels.

3.4 Visual Avatar Experiments

Visual experiments were based on visual psychophysical experiments to measure the threshold values. Three visual experiments (motion detection, angle discrimination, velocity discrimination) were conducted. For all of them, different simulation procedures were executed. However, the structure of the training ground and the objects in it were exactly the same. Figure 3.6 shows the simulation environment and objects. The experimental setup, and interaction path pointed through red arrows in Figure 3.1 were used in visual experiments.

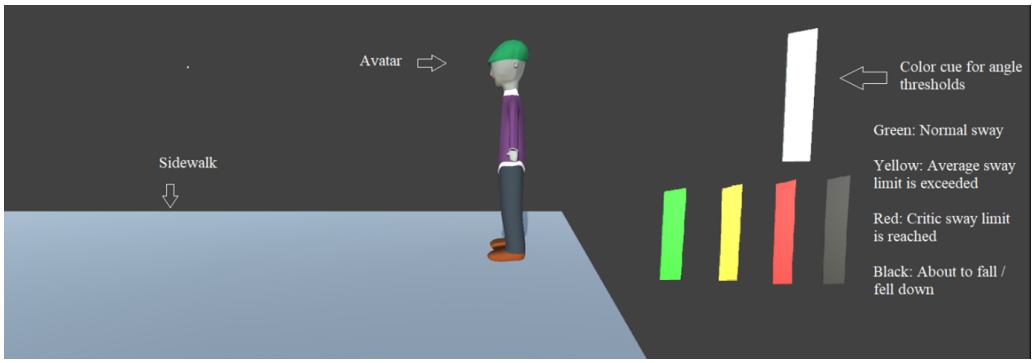

Figure 3.6 The training ground and the objects.

3.4.1 Motion Detection

Motion detection experiment, a two-interval force-choice task is done to measure the absolute threshold of the motion of the avatar. To achieve that, the adaptive tracking method (Yıldız and Güçlü 2013) was used, and the threshold value was set to a 75% probability of detection. In the detailed procedure, two scenes were presented to the participant. In one of the scenes, the avatar rotated about its ankle in either anterior or posterior directions while keeping its hips and knees stationary. In the other scene, the avatar was standing still at the starting point. Scenes order was set randomly. Then, the participant is asked to press one of the rights or left arrow buttons depending on the scene where the avatar was rotating (if first scene left button, other wise right button). The rotation angle decreased by 0.5° with every correct answer until the participant made a mistake or reached the 0.5° threshold. Then, the angle increased by 0.5°(if participant made a mistake), and with every new mistake, it increased by 0.01°. On the other side, after the first mistake or the 0.5° threshold, with three correct answers (they don't need to be consecutive), the rotation angle decreased by 0.01°. When it reached to 0.05° threshold angular increase/decrease changed into 0.0001° The experiment ends if the last 20 stimuli were in the range of ± 0.001°. This procedure is done at four different speeds for both directions separately.

3.4.2 Angle Discrimination

Angle discrimination experiment is a difference threshold measure that provides essential information about the participant's ability to discriminate the smallest difference in the static tilt of the avatar's posture. In the experiment, the constant stimuli method was used. Three reference angles (standard stimulus, SS) were set in the range of the limit of stability, for anterior: 90.5°, 92°, 93.5°, and posterior: 89.5°, 88.0°, 86.5°. The limit of stability was assumed to be between upright position (90°) ±12.5° [14]. Anterior and posterior sessions were done in different sessions to prevent possible confusion caused by closer angles (anterior-90.5°, posterior-89.5°). Eight comparison angles (stimuli) were generated by adding (anterior) or subtracting (posterior) eight angles (0.05, 0.1, 0.15, 0.2, 0.35, 0.5, 2, 3.5) to the standard stimulus to increase the body tilt. In each trial, two scenes were presented to the participant. In one of them, there was the avatar with reference sway and the other one had the avatar with comparison sway. Scenes were presented in pre-determined random order. The participant chose the scene in which sway angle was higher. All reference angles were compared with their comparison angles. Every combination was repeated 20 times. Totally, 480 trials were done for each session. The response of the participant was recorded in real-time. Thresholds were set to a 75% probability of detection.

3.4.3 Velocity Discrimination

The velocity discrimination experiment is another difference threshold measure conducted to calculate the smallest angular velocity difference the participant can discriminate. Three angular velocities (1-2-3 deg/s) were set as reference velocities. We generated comparison velocities by adding five angular velocities (0.1-0.2-0.3-0.4-0.5 deg/s) to reference velocities. Every reference velocity was compared to five comparison velocities of their own. These velocities were set within the normal angular sway velocity range. The procedure was similar to the previous experiment; unlike in experiment two, the avatar was rotating in both scenes, and the participant was asked to select the scene where the avatar was rotating faster. Scenes were presented in random

order. The response of the participant was recorded in real-life. Thresholds were set to a 75% probability of detection.

3.5 Vibrotactile Experiments

Vibrotactile experiments were done to measure motor localization and identification of the avatar's postural information through applied vibrotactile feedback. The experimental setup, and interaction path pointed through green arrows in Figure 3.1 were used in vibrotactile experiments.

3.5.1 Motor Localization

Motor localization experiments were conducted to find the distance between motors that provide the best identifiable placement and to find the best modulation that makes the stimulus the most identifiable. Mixed modulated vibrotactile stimuli localization is the first vibrotactile experiment. It was divided into two session. In the first one, the participant sat in front of a screen, and the experimenter put the armband on the participant's right upper arm in the explained way before. The participant was trained for 1 minute just before the experiment begins. In the training part, vibration motors were activated sequentially one motor at a time and stay on for 1 second, and a 0.5-second break was given between two motor activation. Also, the currently activated motor's number tag was shown on the screen. Unlike the training in the experiment, six vibration motors were activated one at a time in pre-determined random order, and the participant was asked to tell which motor is activated. The vibration motors applied single pulse with 1s pulse-width to the skin. Then, 2-second break was provided to record the participant's answer. Each motor was activated 20 times.

The second session was built based on session 1. The main difference was another stimulus was added. Thus, some parts of the training and experiment procedure were modified accordingly. The new stimulus was formed by two vibrations with 475ms

duration. The interval between vibrations was 50ms. Before the trials begin, the participant did the training to learn how to identify motor locations and stimulus types by tactually sensing them. As in the previous training procedure, motors were activated in order. However, this time 0.5 seconds after the first stimuli (single pulse with 1s pulse width) second stimuli (two pulses with 475ms pulse width and 50ms interval in between) was applied. The number of the motor and stimuli form was presented on the screen. At the end of the training, trials began. This time the participant had to find the motor location and stimuli form. Each motor was combined with each stimulus (6 motors x 2 stimuli) and all combinations were applied to the participant 20 times in pre-determined random order.

Later on, we changed the modulation type to pulse number modulation. To provide that, first, we created small pulses with 50ms pulse width by turning on and off the vibration and generated pulses in numbers that we wanted to generate. The interval duration between pulses was set to 50ms same as in previous experiment. The experiment was completed in two sessions. In the first session, we generated stimuli at three pulse number (4-7-10) and trained the participant in three pulse numbers. Each motor were activated depending on the pulse number (4-7-10) in serial order for the training purposes. In the experiment, procedure was same as the mixed modulation. we applied each stimuli 20 times for each motor in random order. In the second session, same procedure is done by only using two pulse numbers (4-10).

At the end of the experiments, distance between motors were set to a point that provides best localization (81.2%). Also different stimuli modulations were compared to find the best modulation which can provide better localization. As a result, Pulse-number modulated stimuli provided better localization than the Mixed modulated stimuli (81.2%-81.1%).

3.5.2 Avatar Identification with Pulse Number Modulated Vibrotactile Feedback

After localization experiments we started the identification experiments. This was the part that certain vibrotactile stimuli were matched to avatar's postural positions based on the physiological values [14]. First, a small experiment were designed similar to second session of the pulse-number localization experiment to train the participant before proceeding to identification experiment. However, this time, activation of motors with higher numbers also activated the motors with lesser numbers. For example, if AREM2 was activated, AREM 1 was also activated, but AREM3 remained off. However, if AREM3 activates, AREM2 and AREM1 will be activated. That way we created amplitude levels (Anterior/Posterior level1-2-3) of stimuli. For pulse numbers we only used 4 pulse and 10 pulse to encode the slow and fast velocity. In the training part of the experiment, for each pulse number, motors were incrementally recruited first anterior motors then the posterior motors and participant saw the amplitude levels and pulse numbers on the screen. In the experiment, anterior and posterior motors were activated in random amplitude levels with random pulse number. At the end of every trial we asked participants to tell what was the amplitude level in which direction and what was the pulse number. As in the previous experiments, results were recorded in real-time.

In the identification experiment, the vibrotactile stimuli represented specific postural sway angles at specific angular velocities. The amplitude of the stimuli represented the particular angles of the sway, and the number of the stimuli represented specific angular velocities of the sway. Figure 3.7 shows the special positions and velocities. Posture sways and velocities were set based on the physiological range mentioned in the literature [14]. Table 3.1 and Table 3.2 shows the assigned amplitude/Pulse-number values for sway angle/velocity values.

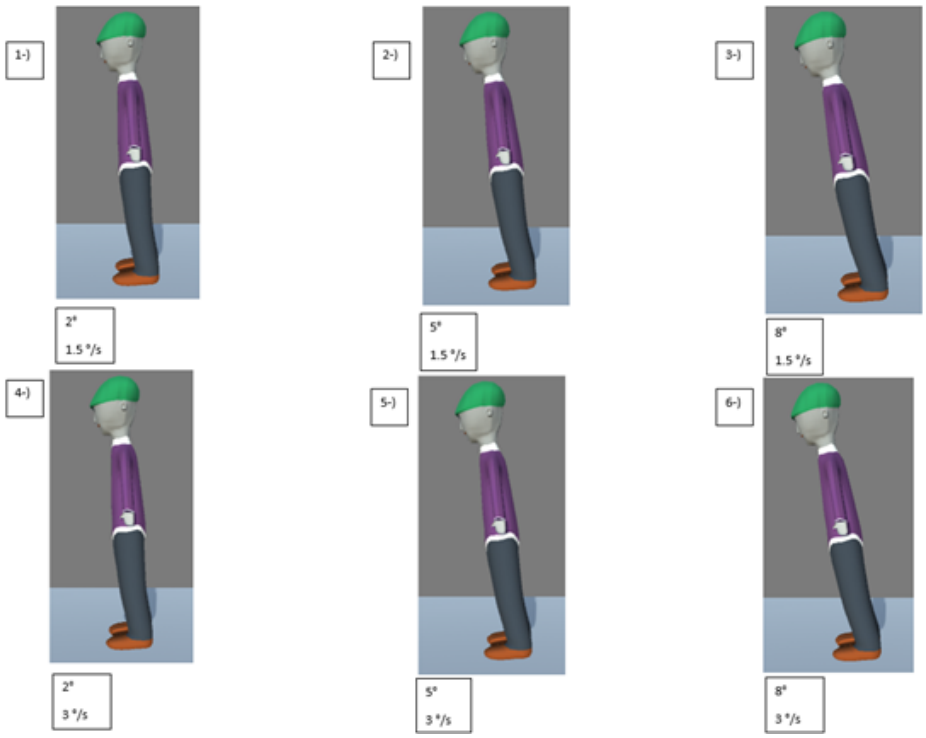

Figure 3.7 Velocity-angle combinations used in the anterior session.

Table 3.1
Configurations of the anterior postural conditions.

Posture Sway(°)	Angular Velocity(°/s)	AREM Amplitude level	Modulation pulse-number
2	1.5	1	4
5	1.5	2	4
8	1.5	3	4
2	3	1	10
5	3	2	10
8	3	3	10

In training, vibrotactile stimuli for both anterior and posterior were applied to the participant sequentially while participant were looking at the relevant image on the screen. After the training, the screen was turned off and vibrotactile stimuli were applied in pre-determined random order and the participant were asked to match the stimuli with the correct choice (Figure 3.7). The purpose of this experiment is

Table 3.2
Configurations of the posterior postural conditions.

Posture Sway(°)	Angular Velocity(°/s)	PREM Amplitude level	Modulation pulse-number
2	1.5	1	4
5	1.5	2	4
8	1.5	3	4
2	3	1	10
5	3	2	10
8	3	3	10

to understand the which vibrotactile stimuli were identified for postural conditions. Because, this configuration was designed to be used in the parkour experiment.

3.6 The Parkour for Simulated Road Crossing

This is the last conducted experiment of the thesis. The experimental setup and interaction path highlighted through black arrows in Figure 3.1 were used in that experiment. Its design was based on a real-life scenario and its configurations were set depending on the collected data in previous experiments and physiological limitations [14]. The experiment was divided into two parts. In the first part, the avatar was standing at the traffic lights for approximately 180 seconds + duration of sways. Meanwhile, It had randomly occurred anterior and posterior sways at different angular velocities (2 sway in 3 seconds, time during the sway is excluded). When it reached particular sway angle thresholds (2-5-8), vibration motors were activated, as mentioned in identification experiment. After 120 sways (60 anterior and 60 posterior sway), the second part began, and it started to walk forward. The avatar continued to sway as it walked. After another 120 sways, the session was completed. Avatar's sway occured at two different angular velocities (1.5 deg/s, 3 deg/s) In the training part, a color cue that hints at the current zone the avatar is in was added (Figure 3.6). The participant

could not interfere the avatar's sway between 0° to 2° because, we assumed that was the normal sway range [53] and cue remained in green color. After 2 degrees, the cue color turned into yellow. The yellow color means that the avatar reached the first color transition by passing the normal sway range and entered the preferred zone (2°-5°) also known as yellow zone. The participant is asked to interfere with the avatar's sway in that zone. The red color means, the avatar is in the critical zone (5°-8°) also known as red zone, and the participant is asked to act fast in that zone. And finally, the black color means the avatar reached the black zone (8°-10°) and it is about to fall less than a second. It is essential that the participant had to watch the avatar closely because as the experiment began, there was no cue; the participant's task was to press the button leading to sway direction as soon as the avatar reached the first color transition to correct avatar's posture. However, he could press the button anytime from the first transition to fall (2°-10°). The experiment was repeated three times with different stimulus configurations. First, participants only had visual feedback and press the buttons accordingly. Then participant had only tactile feedback. He completed the experiment blindfolded. In the last session, he had both vibrotactile and visual feedback.

4. RESULTS

Eight different experiments were conducted for a single participant. Based on their methods, these experiments were classified into three main groups (visual experiments, vibrotactile experiments and the parkour experiment).

4.1 Visual Experiments

4.1.1 Motion Detection

Eight absolute thresholds are measured in eight sessions with different parameters with adaptive tracking. In every trial, the participants must press the arrow key to choose the scene with rotation. Results can be seen in table A.1 and A.2. The first row shows the velocity and direction parameters, and threshold values depending on the parameters above are listed in the second row. Angular velocity range is set according to physiological values in literature [53]. However, the angular velocity of the avatar can't exceed 2dgs/sec. Otherwise, rotations smaller than 0.003 degrees can't be generated because of the software limitations. In Figure 4.1, for each velocity, there are two bars. The blue one on the left represents the anterior threshold, and the orange bar on the right represents the posterior threshold. Thresholds are set to a 75% probability of detection.

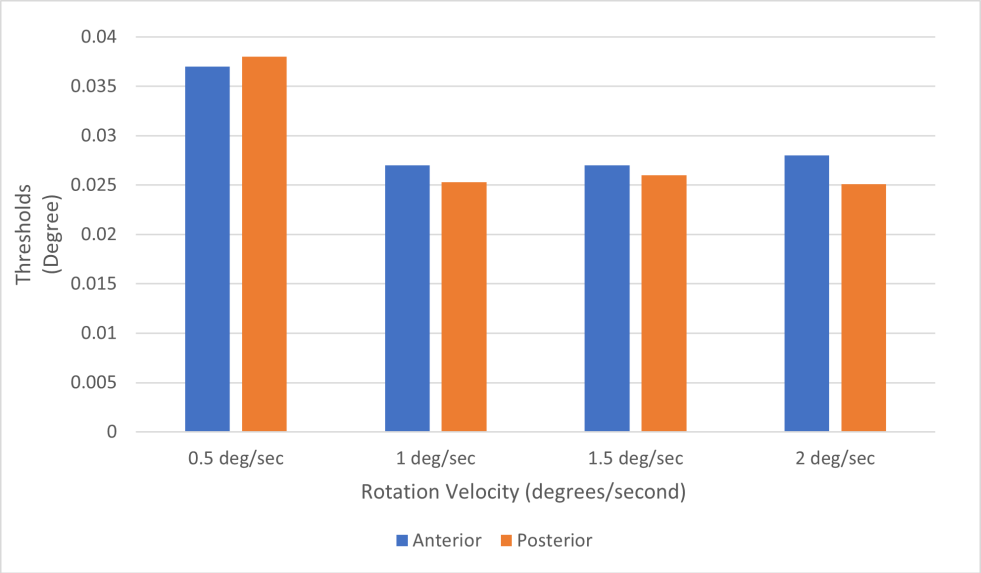

Figure 4.1 Threshold values of the Motion Detection Task.

4.1.2 Angle Discrimination

After the motion detection, the angle discrimination task was conducted to measure the difference thresholds on three reference points for anterior-posterior directions by the method of constant stimuli. Participants were trained before the experiment according to the procedure. In contrast to the first experiment, the participant compared the two pictures and chose the one where the avatar had a higher angle sway. The experiment was completed in two sessions, one for each direction. Three reference rotations (anterior:90.5°, 92°, 93.5°, posterior: 89.5°, 88.0°, 86.5°) were compared with new rotations. New rotations were generated by adding five additional angles to each reference. 20 trials for 15 combinations were executed in two directions. Measured data were fitted to sigmoidal psychometric functions and the thresholds were set to 75% probability of discrimination. the Detailed experiment results were shown in Table A.3-4, and approximate difference thresholds were shown in Figure 4.2. Positions in the Figure are the reference angles and presented in the Table A.3 for the anterior and Table A.4 for the posterior.

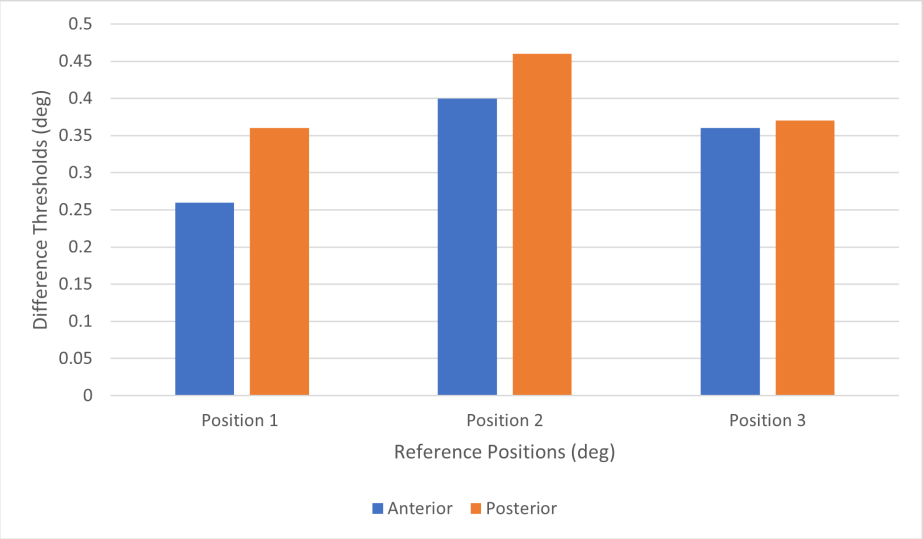

Figure 4.2 Threshold values of Angle Discrimination.

4.1.3 Velocity Discrimination

In the velocity discrimination experiment, difference thresholds were measured for each reference velocity through the method of constant stimuli. Three reference velocities (1-2-3 deg/s) were set and compared to their comparison velocities. The participant was asked to find the scene where the avatar rotates faster. Measured data were fitted to sigmoidal psychometric functions and the thresholds were set to 75% probability of discrimination. Approximate anterior and posterior thresholds were shown in the Figure 4.3. Correct answers for anterior and posterior session were presented in Table A.5-6.

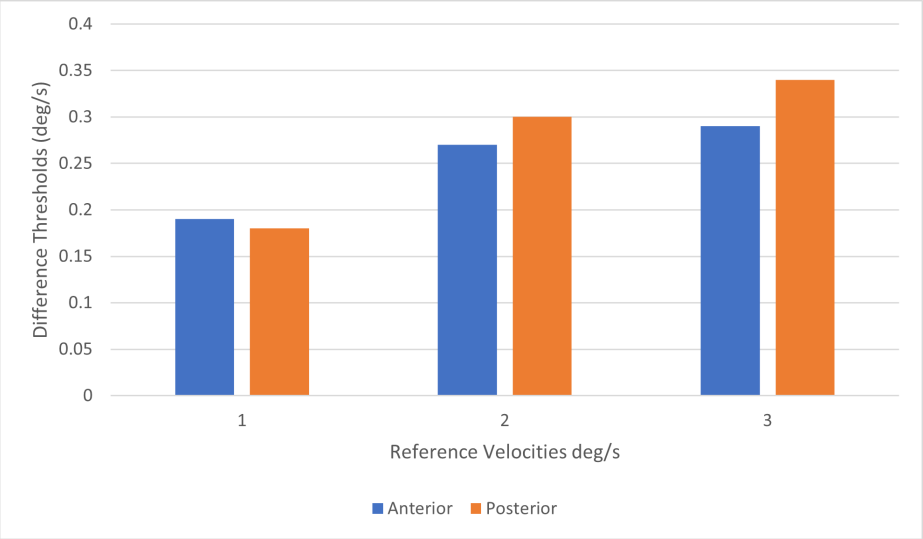

Figure 4.3 Threshold values of Velocity Discrimination.

4.2 Vibrotactile Experiments

4.2.1 Motion Localization Experiments

Motor localization experiments were conducted in two experiments. The first was done to measure localization of the vibration motor with mixed modulated vibrotactile feedback. Before the experiment, the participant was trained in an ordered sequence (1-2-3-4-5-6). Then, vibration motors were activated in pre-determined irregular order, and the participant told the motor number that he believed to be activated. As mentioned in the methods, motors 1-3 (AREMs) were designed to encode the anterior rotations of the avatar, and motors 4-6 (PREMs) for the posterior rotations. Figure 4.4 shows the confusion matrix generated by the experiment results.

Rows show the actual answers for each class, and the columns show the participant's responses. The participant only localized Motor1 as all correct. He made the most of the mistakes while identifying the Motor3. Specifically, he confused AREM3 with AREM1 and AREM2 too often. Also, precision, recall, f1, and accuracy scores were calculated according to the confusion matrix. In this study, we considered recall score provides more crucial information than the precision score. The recall scores

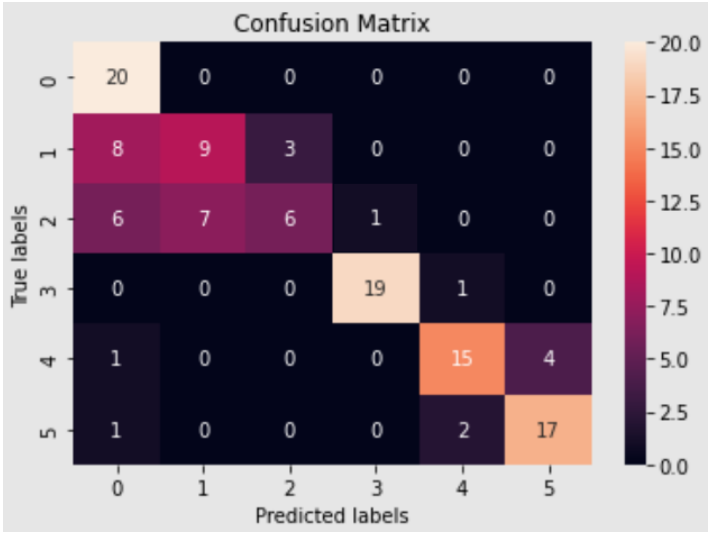

Figure 4.4 Confusion Matrix of mixed (single pulse) modulated vibrotactile stimuli localization. Class 0-1-2 are AREM (1-2-3) localizations, Class 3-4-5 are PREM (1-2-3) localizations. Numbers in the matrix are counts in 20 trials.

exceeded 75% while identifying motors: 1-4-5-6. The participant showed the worst performance while identifying Motor3 (AREM3) with a 35% recall. The participant was able to identify Motor 2 slightly better than Motor3. However, both Motor2 and Motor3 have less than 50% recall overall. The accuracy of the first session is 73%. Detailed precision, recall, f1 scores of the classes were shown in the Figure A.7.

Table 4.1
Shows the precision, recall, f1, accuracy scores of mixed (single pulse) modulated vibrotactile stimuli localization.

Precision	Recall	F1	Accuracy
0.74	0.72	0.71	0.73

The second session was conducted right after the first one. In addition to the first one, the participant tried to localize applied stimuli and the pulse number (single or double). First six class in confusion matrix (Figure 4.5) are vibration motors activated with single pulse stimuli and last six are activated with double pulse.

Second session's results were listed in Figure 4.5 The participant didn't make any mistakes while localiztion stimuli applied through the AREM1 at both pulse numbers. AREM3 localization had the lowest correct answers at both pulse numbers. The

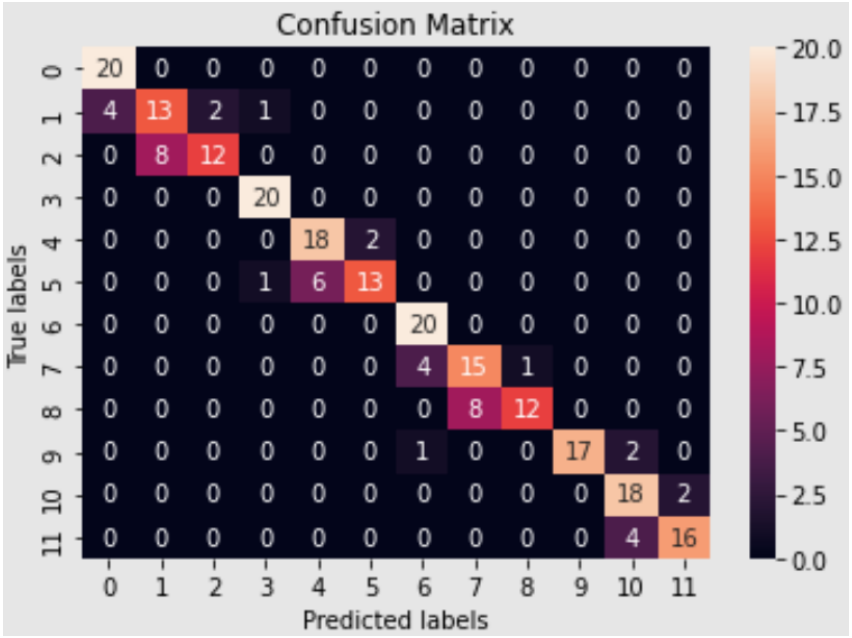

Figure 4.5 Confusion Matrix of mixed (single/double pulse) modulated vibrotactile stimuli localization. Class 0-1-2 are AREM (1-2-3) localizations with single pulse, Class 3-4-5 are PREM (1-2-3) localizations with single pulse. Class 6-7-8 are AREM (1-2-3) localizations with double pulse, Class 9-10-11 are PREM (1-2-3) localizations with double pulse. Numbers in the matrix are counts in 20 trials.

recall score of AREM1 was 100% for both pulse number. Nevertheless, recall scores of AREM2 and AREM3 exceeded 50%, unlike before. AREM1 and PREM1 were the most localizable motors in their groups. The overall accuracy of the second session was 81%. Detailed precision, recall, f1 scores of the classes were presented in the Appendix (A.8).

Table 4.2
Shows the precision, recall, f1, accuracy scores of mixed (double pulse) modulated vibrotactile stimuli localization.

Precision	Recall	F1	Accuracy
0.82	0.81	0.80	0.81

For both mixed modulated vibrotactile feedback configurations, the chi-square test results showed p smaller than 0.05. Thus, predicted values and actual values were significantly dependent. Also, we compared the results of procedures one and two through the z test and they were not significantly different. Class recalls and experiments accuracies for both sessions were far above the their chance levels (16,667%,

8.33%).

Then, we have conducted the localization experiment with only pulse number modulated vibrotactile feedback. Experiment was repeated two times with different configurations. The participant was trained in serial order (Motor1-4pulse, Motor1-10pulse. . . Motor6-4pulse, Motor6-10pulse). Results of the session with two pulse number (4 and 10) were shown in Figure 4.6. Class 1 to 6 are vibration motors (AREM1-2-3, PREM1-2-3) activated with 4 pulse and other 6 are the motors activated with 10 pulse. PREM3 had the lowest class recall with 65% on 4 pulse and 50% on 10 pulse, and the overall accuracy score is 81%. Figure A.9 shows the detailed precision, recall, f1 scores of the classes.

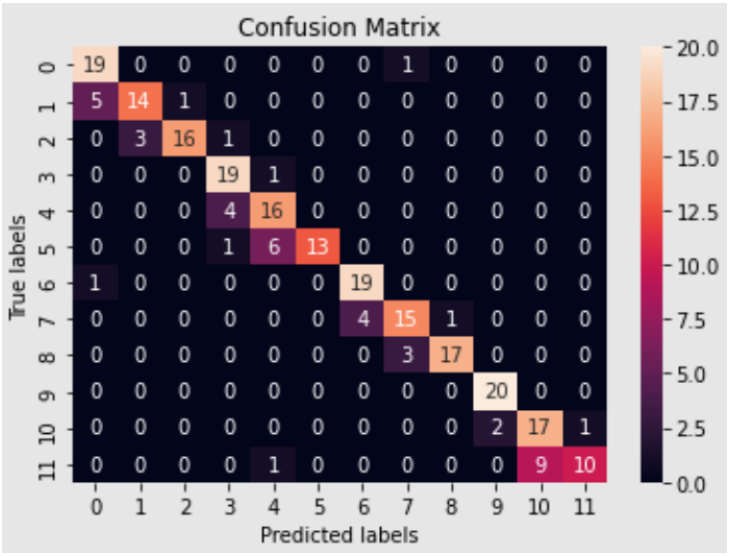

Figure 4.6 Confusion matrix of pulse-number modulated vibrotactile stimuli localization in two pulse number. Classes 0-5 are AREMs and PREMs localization at 4 pulses and 6-11 are localization at 7 pulses.

Table 4.3
Precision, recall, f1 and accuracy scores of pulse-number modulated vibrotactile stimuli identification in two pulse number.

Precision	Recall	F1	Accuracy
0.83	0.81	0.81	0.81

Results of the session with evenly spaced pulse numbers (4-7-10) were showed in the next Figure 4.7. Before the session, the participant was trained again with the

same logic as in the training part of session 1. The only difference was between 4 pulse and 10pulse; 7 pulse stimulation was applied. Classification method was similar to previous session. Only difference was Classes between 7-12 were motors activated at 7 pulse stimuli and last six classes represented the 10pulse stimuli.

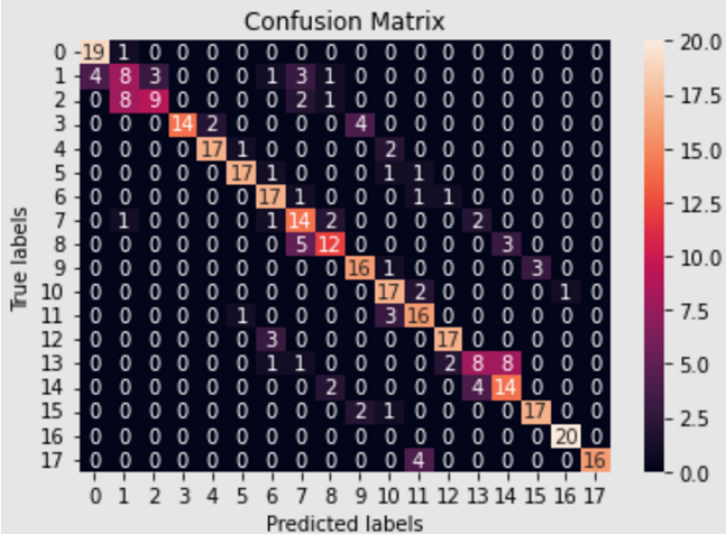

Figure 4.7 Confusion Matrix of pulse-number modulated vibrotactile stimuli identification in three pulse number. Classes 0-5 are AREMs and PREMs localization at 4 pulses, 6-11 are localization at 7 pulses and 12-17 are localization at 10 pulses.

This process decreased the accuracy of all motor identifications. AREM2 had the lowest 4 pulse, 10 pulse recall score with 40%, and AREM3 has the most inadequate 7 pulse recall. The overall accuracy of session 2 was 74%. Detailed version of precision, recall, f1 scores of the classes were presented in the Figure A.10.

Table 4.4
Precision, recall, f1 and accuracy scores of pulse-number modulated vibrotactile stimuli localization in two pulse number.

Precision	Recall	F1	Accuracy
0.75	0.74	0.74	0.74

According to the chi-square test (p smaller than 0.05), actual values and predicted values were significantly dependent for both sessions. Results of pulse-number modulation sessions (2 pulse and 3 pulse) are not significantly different according to

the z test score (p greater than 0.05). Class recalls and experiments accuracies for both procedures are far above the their chance levels (8.33%,5.56%).

4.2.2 Avatar Identification Experiment

In this section the participant matched the vibrotactile stimuli with visual avatar's postural conditions. Before the identification experiment we conducted a short experiment to train the participant for the amplitude changes. The training experiment was almost identical to pulse number modulation experiment (2 pulse). The only differences were that motors were not activated one at a time but recruited incrementally, and two sessions were executed for AREMs and PREMs separately.

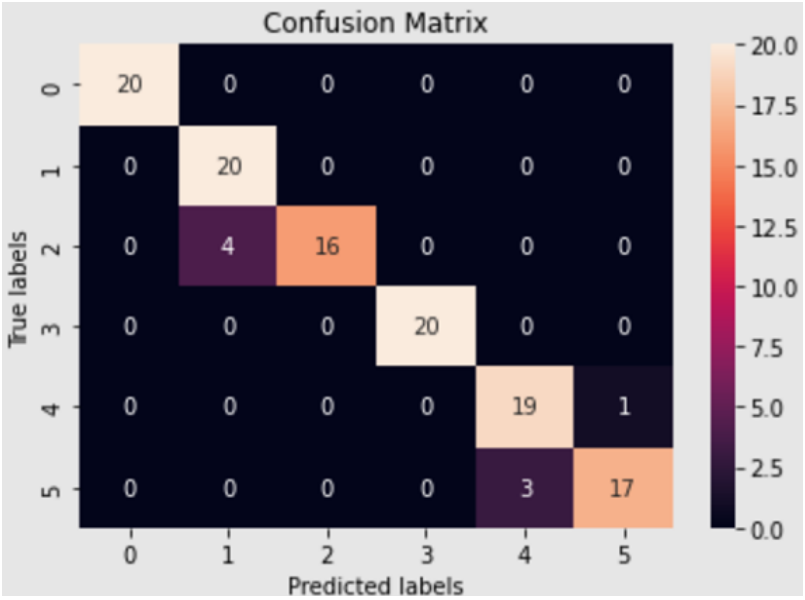

Figure 4.8 Confusion matrix of training of the incrementally recruited pulse-number modulated vibrotactile stimuli identification for anterior rotation. Classes 0-2 represents the amplitude level 1-3 at slow angular velocity, and 3-5 represents the amplitude level 1-3 at high velocity.

Detailed results were listed in Figure 4.8 confusion matrix. For anterior motors, the participant identified level1 and level2 at 4 pulse and level1 at 10 pulse as all correct. Most of the mistakes were caused by confusion between level2 and level3. For both pulse numbers, he mistakenly classified the some of the level3 stimuli as level2 stimuli. According to Table 4.6.1, both recall scores of level1 of the anterior and posterior motor groups are 100%, and overall accuracies are 93.33% and 91.66% for the anterior and

posterior groups. level2 has the lowest recall score at 80%. The accuracy score of the anterior session is 93%.Detailed precision, recall, f1 scores of the classes were presented in the Figure A.11.

Table 4.5
Precision, recall, f1 and accuracy scores of training of the incrementally recruited pulse-number modulated vibrotactile stimuli identification for anterior rotation.

Precision	Recall	F1	Accuracy
0.94	0.93	0.93	0.93

The same procedure was applied to the posterior motors in the next session. Identification results were presented in Figure 4.9 The confusion matrix shows that the participant could identify level1 without trouble at both pulse numbers.

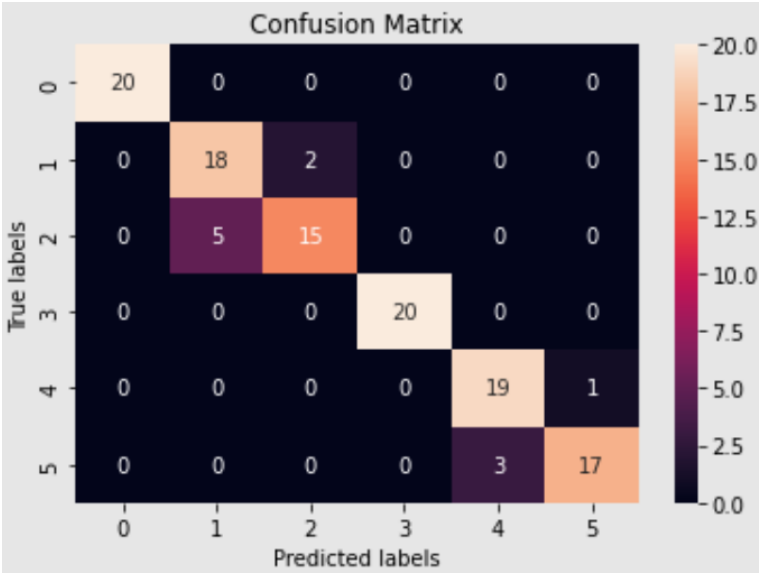

Figure 4.9 Confusion matrix of training of the incrementally recruited pulse-number modulated vibrotactile stimuli identification for posterior rotation. Classes 0-2 represents the amplitude level 1-3 at slow angular velocity, and 3-5 represents the amplitude level 1-3 at high velocity.

The highest number of mistakes occurred when identifying level3 at both pulse numbers. Thus, level1 at both 4 and 10 pulse has the highest recall score with 100%, and level3 has the lowest recall score with 75% at 4 pulse. The accuracy of the posterior session is 91% Detailed precision, recall, f1 scores of the classes were shown in the Figure A.12. Actual values and predicted values were significantly depended depending on the chi-square test (p smaller than 0.05) for both sessions. Two proportion Z test between

Table 4.6
Precision, recall, f1 and accuracy scores of training of the incrementally recruited pulse-number modulated vibrotactile stimuli identification for posterior rotation.

Precision	Recall	F1	Accuracy
0.91	0.91	0.91	0.91

anterior and posterior session shows that there is no significant difference between them. Finally, both sessions were greater than the 16.667% chance level.

After that, we coducted the avatar identification experiment. Vibrotactile stimulus configurations in training experiment were bound to specific visual avatar conditions. The participant was trained until he was ready. Then he was asked to match the coming vibrotactile stimuli with avatar positions that appeared on the screen. Two sessions were conducted in anterior and posterior directions. Accuracy scores for anterior are listed in table 4.7 The participant showed 100% recall in level 1 for both pulse numbers, and the lowest recall of anterior is 80%. Figure 4.10 is the confusion matrix of the anterior session. Diagonal cells show the correct answers for each configuration.Detailed precision, recall, f1 scores of the classes were presented in the Figure A.13.

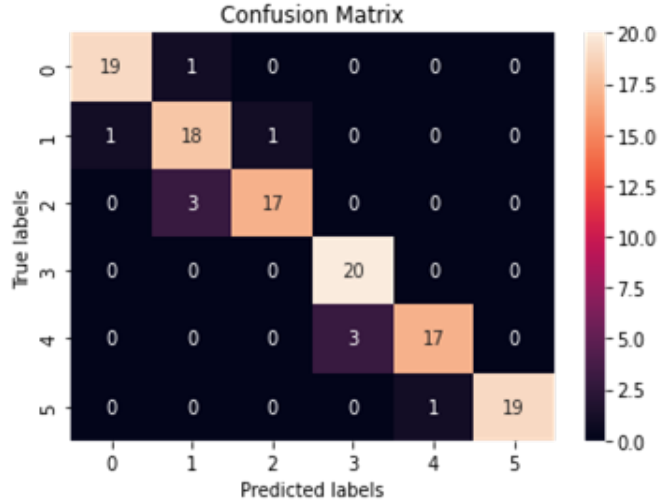

Figure 4.10 Confusion matrix of gathered results from the anterior session of visual avatar identification experiment. Diagonal cells show the correctly answered results. Classes 0-2 are sway angles of visual avatar (2-5-8) at 1.5 deg/s and others are sway angles at 3 deg/s.

Table 4.7
Precision, recall, f1, and accuracy scores of the anterior session.

Precision	Recall	F1	Accuracy
0.92	0.92	0.92	0.92

For the posterior session, Figure 4.11 shows the confusion matrix of the posterior trials. The participant made no mistakes about pulse number in both anterior and posterior. He just made mistakes in identifying the juxtaposition of amplification levels.Accuracy results are presented in Table 4.8, and the best performance with 100% recall was measured when identifying level2Fast stimuli. Detailed precision, recall, f1 scores of the classes were presented in the Figure A.14.

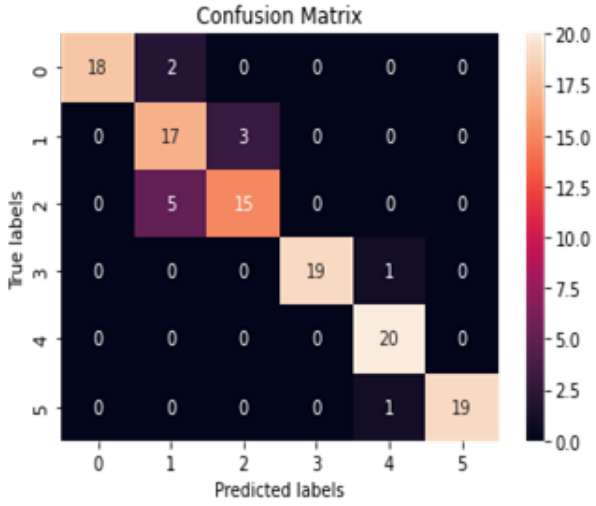

Figure 4.11 Figure 4.7.2 Confusion matrix generated from the data recorded in the posterior session of visual avatar identification experiment. The diagonal path shows the correct answers made by the participant. Classes 0-2 are sway angles of visual avatar (2-5-8) at 1.5 deg/s and others are sway angles at 3 deg/s.

Table 4.8
Precision, recall, f1, and accuracy scores of the posterior session.

Precision	Recall	F1	Accuracy
0.91	0.90	0.90	0.90

As in the previous experiments, p value is smaller than 0.05 for both sessions, according to the chi-square test. So, predicted and actual values are significantly

dependent. Also, the results of the anterior and posterior sessions are not significantly different. All classes in both sessions are far above the 16.667% chance level. Results taken from the plot experiment were adequately promising for further studies.

4.3 The Parkour Experiment

In the parkour experiment, a real time scenario was designed mentioned in the method part. Before the beginning of the experiment, the participant was trained with a cue that provides information about the positional condition of the avatar until he learns the experiment. The experiment was repeated three times with three different feedback configurations. The participant was asked to stop the avatar in one of the three zones, preferably in the yellow zone (preferred zone). Other zones were the critical zone and the falling zone. The success criteria depended on the end zone are shown in table 4.9.

Table 4.9
Success criteria of the experiment. Colors represents the sway angle range for classification and criteria shows the classes.

End zone	Success Criteria
Yellow	Number of Responses
Red	Number of Responses
Black	Number of Responses
Fall	Number of Fall

In the first session, the participant only had visual feedback by watching the avatar rotates at different velocities. In the standing part, Avatar was standing at the start point of the parkour, and it was having predetermined randomly occured angle sways (either anterior or posterior) twice in three seconds until the beginning of the walking part. The participant was supposed to stop the avatar before it fell. Table 4.10 shows the results of the completed trials. The participant intercepted the avatar 115 times in the yellow zone (preferred zone) and 5 times in the red zone (critical zone). Avatar never reached the black zone or the falling zone. The participant had a 95.8% yellow zone score and a 3.2% red zone score. Then, the avatar started to walk at 1m/sec, and the participant's task was the same. As a result, The participant has a 100% yellow zone score, which means he stopped the avatar in all trials while inside the yellow zone. Walking score is also shown in Table 4.10.

Table 4.10
Results of the first session (only visual). Numbers indicate how many trials were completed in what zone.

Color/Action	Standing	Walking
Yellow	115	120
Red	5	0
Black	0	0
Fall	0	0

In the next session, the participant repeated the session blindfolded. He only had tactile feedback. The procedure was the same as the previous session. In the standing part, the participant stopped the avatar 112 times in the yellow zone, seven times in the red zone, and one time in the black zone (falling zone). Participant stopped the avatar 93.34% in yellow zone, 5.83% in red zone, and 0.8% in black zone. In the walking part, the participant gets the lowest yellow zone score of the entire experiment by 90.83%. And he had 9.17% number of responses in red zone.

Table 4.11
Results of the second session (only tactile).

Color/Action	Standing	Walking
Yellow	112	109
Red	7	11
Black	1	0
Fall	0	0

In the final session, both tactile and visual feedback was applied to the participant. The goal of the participant was the same as in the sessions before. According to the results in Table 4.12, the participant showed a remarkable performance. In the standing part, he had 99.16% yellow zone and 0.834% red zone scores. In the walking part, the yellow zone score was 98.33%, and red zone score was 1.67%. Finally, feedback strategies are compared between each others by Z test and results showed that there is not significant difference between those strategies.

Table 4.12
Results of the third session (visual and tactile).

Color/Action	Standing	Walking
Yellow	119	118
Red	1	2
Black	0	0
Fall	0	0

5. DISCUSSION

5.1 Previous Studies

Virtual Reality is a progressive concept that can make designing exclusive training methods possible in many fields. Etienne van Wyk et al. designed virtual mining safety training to prevent mine accidents caused by procedural violations. To provide that, first, they did a detailed investigation of mine structure, safety protocols, and frequently occurred accidents by observing the field during work hours and surveying miners, engineers, and safety specialists. The workers took informal training in the mine's training center. According to the extracted data, they recreated the virtual mine and designed different scenarios for the experiment. In those scenarios, there were different procedural violations or problems that occurred, and recruited participants among workers were asked to choose the correct violation or way to fix the problem between given options. That provided a safe environment to test and reinforce the safety training. Also, researchers added some realistic clips about what happens if they choose the wrong answers [54]. In our study, we did not train the participant outside of the virtual environment, but we provided virtual training program for the incoming experiments. Another virtual reality-based study is done by Jeffrey Jacobson. They designed an immersive virtual environment that can make people design balance disorder rehabilitations. First, they built an isolated safe physical area with multiple devices, such as a treadmill, force plate, head and eye trackers, motion sensors, and life functions monitor. Participants can be grappled to the environment through a parachute harness. Visual content is projected to the environment dynamically depending on the participants' field of view. Participants' head and eye motions are tracked by cameras and sensors. Two different views are projected, one for the right eye and the other for the left eye. Participants will wear polarizing glass to mix the views and provide a 3D image. As a result, they developed an adjustable integrated system that can be used to design several balance rehabilitation procedures [55].

Vibrotactile feedback is a popular method to provide information about different conditions to users. For example, patients with balance disorders cannot maintain balance or postural orientation independently. Therefore, they can be guided to regain their postural control through external sensory feedback like vibrotactile feedback. In literature, there are many studies were conducted to achieve that purpose [1, 11, 56]. One example, Wall and Kentala developed a vibrotactile feedback belt for people suffering from postural deficit. They also recorded the participants' current body tilt through an accelerometer and gyroscope placed back of the belt. Their study showed that vibrotactile feedback reduced the recovery time, peak deflection, and anterior-posterior body sway. However, applying vibrotactile feedback at the belt level may result in insufficient sensation even though applied stimuli are suprathreshold. In our study, to prevent that issue, we applied the stimuli to the right upper arm of the participant. Another study by Seinko et al. used a trunk-based vibrotactile feedback system to improve balance in vestibular deficit patients during locomotor activities. First, they placed a vibrotactile feedback device on the trunk of patients vertically and an inertial measurement unit on the patient's lower back. While the patients were walking with increasing body sway, tactors were activated. As a result, they reduced the medial-lateral sway during complex locomotor activities. Also, they did a survey about the confidence level of participants' current conditions, and the results showed they stated that they were more confident while they were using the vibrotactile device [57]. Goebel and his team designed a vibrotactile feedback system that applies the stimuli through a head-mounted device to prevent the fall risk of patients. They trained their participants and conducted experiments in real-life. According to their results, they decreased the fall number of the patients by 40% (90% - 50%). In our study the participant completed the task without a fall. However, our task did not involve any physical challenges for now. To make a more accurate comparison we have to use the system in real world with patients.

5.2 Technical Limitations and Other Issues

The lack of budget for the project prevented us from using the head-mounted display device for the virtual reality part. Because of that, we could only present the virtual environment through the laptop screen. As a result, we could not isolate the participant from the real world entirely. Also, we could only provide a third-person view for the participant. As for the modeling, creating a realistic model takes lots of time and expertise. In our team, there was no member who could provide that kind of support. Thus, we tried to use already existing assets in Unity3D's asset library. Unfortunately, those assets had unrealistic and distracting animations and textures. Therefore, the entire model and environment are designed by author. In the vibrotactile armband part, we couldn't calibrate the vibration motors. Because thesis work was not performed in laboratory environment, and motors were not suitable for calibration. Also, the frequency and the amplitude of the vibration motors were voltage-dependent and can't be configured separately. Thus, we set input voltage 3.3V to get discriminable, non-noxious suprathreshold stimuli. The delay of the driven stimuli was changing depends on the communication velocity between Arduino and Unity3D. At the beginning of some experiments, sessions had to be repeated due to minor communication errors. Other than the technical issues, we could not find any participants to try the procedure due to the global pandemic. So, we converted the study to a proof of concept and tested the procedure only on the experimenter.

5.3 Future Work

This study may be considered as a first step of a larger project. After that study, thesis author is planning to conduct similar work in clinical setting. On the procedure side, we are planning to improve both virtual reality training and vibrotactile feedback parts. In the virtual reality training part, from now on, we are going to use the HMD set to isolate the participant fully. Models are going to be redesigned more detailly and more realistic. For the comparison, I will duplicate the related experiments and

apply the laws of biomechanics and physics to the objects and environment.

In the vibrotactile feedback part, we are going to convert the system into a wireless design by using a Bluetooth modulator (Zigbee). Also, we are going to add another armband to encode the lateral sway. This design was not made for only virtual training purposes. So, we will design an accelerometer and gyroscope based, real-time postural sway angle/velocity measuring device. Through that device, micro-controller will calculate the angle and velocity in high accuracy and drive the vibration motors accordingly. We are going to attach the device to a flexible belt to measure sway properties from the lower abdomen. Also, patients will be able to use device without any difficulties. To expand the functions of the device, we are going to sync it with the mobile application. That way, in the face of a potential problem such as falling, the application can call for help or collect the sway data during daily activities for further customization.

5.4 Conclusion

In that thesis, I developed a vibrotactile feedback system for people suffering from balance disorders and adjustable training procedures for the feedback system in virtual reality. Balance disorders are serious problems that negatively affect daily activities. Many balance problems are caused by the lack of sensory information result from neurological or vestibular diseases [4]. Providing postural information through vibrotactile stimuli is a promising method used in the literature. [15, 16, 57].

A new method was developed by the author to apply vibrotactile stimuli. First, a simple flexible armband that is adjustable on the arm was designed. We integrated it with six vibration motors, three motors for each direction (AREMs/PREMs). Motor groups were placed on opposite sides of the armband in a crescent formation. To conduct the trials, the armband was placed on the upper arm of the participant where a high sensation can be provided without stimulating the joint receptors. Distance between motors was calibrated through a localization test and set to 1/12 of the upper

arms width. The configuration of the vibrotactile stimuli is another important issue in providing a discriminable and effective sensation. In previous studies, researchers tried to achieve that by applying the 250 Hz suprathreshold vibrotactile stimuli through a belt or head-mounted stimulator [15, 58]. In our work, we compared two modulation types: mixed modulation, pulse-number modulation. According to the result, pulse-number had slightly higher accuracy (81.2%). Therefore, we used Pulse-number modulation in identification and the parkour experiments. Arduino UNO was used to control the application of stimuli. Because it is low-cost, persistent, and compatible with multiple hardware and software [44]. No matter how effective the applied method is, participants must be trained well to use the device [59]. Thus, we designed a training program in virtual reality. Objects, environment, and the representative customizable avatar were designed in Blender. Then, Unity3D was used to design the simulations. To obtain the psychophysical limits, we measured the absolute thresholds (75% probability of detection) at different angle velocities in the motion detection experiment and difference thresholds (75% probability of discrimination) in the angle discrimination and velocity discrimination experiments. According to the results, the participant can detect rotations larger than 0.04 deg/s for both anterior and posterior rotations at all tested velocities. Also, the average difference threholds for anterior/posterior angle discrimination is 0.37 degrees, and velocity discrimination is 0.26 deg/s. These values are far below the sway range that we used in the parkour experiment. Then, vibrotactile stimuli are matched to certain body tilt angle and velocity combinations. For example, 4 pulse level1 stimuli activated at 2 degrees anterior or posterior body sway while the rotation velocity was 1.5 deg/s. In identification experiment, the participant was asked to match the applied stimuli to the image with the correct tilt sway angle and velocity. Participant completed the sessions with 92% accuracy for anterior and 90% for the posterior. Last experiment was designed in a game concept. The task of the participant was to maintain the balance of the avatar by pressing the button in the same direction with the body sway after the avatar reached the first color transition and before the avatar reaches the second color transition. The experiment was repeated three times with different feedback configurations. First, the participant finished the task by only having visual feedback then, by only having vibrotactile feedback, and finally visual and vibrotactile feedback are provided simultaneously. Average success

rate was the 96.2%. Participant showed the best performance with both feedback on (yellow zone scores: 99.1% standing, 98% walking) and worst performance with only tactile feedback on (yellow zone scores: 93.3% standing, 90.8% walking). In this thesis, we designed a vibrotactile feedback device and provided postural data successfully. To train the patients an educational program was created in virtual reality and successfully implemented that for the participant. According to the results, the participant successfully identified the vibrotactile feedback and matched conditions successfully.

This thesis brings two essential novelties to the literature. First, instead of experimenting the vibrotactile balance guidance procedures in real life, participant might experience the procedure in safe virtual reality environments with the 1st or 3rd person views and can have the tactile feedbacks that was designed to be used in real-life scenarios to adjust them without a physical effort. Second, we designed a new, configurable and highly identifiable vibrotactile feedback system with novel modulation patterns. We believe that both vibrotactile feedback and training procedures will be beneficial for patients with balance disorders.

REFERENCES

1. Goebel, J. A., B. C. Sinks, B. E. Parker Jr, N. T. Richardson, A. B. Olowin, and R. W. Cholewiak, "Effectiveness of head-mounted vibrotactile stimulation in subjects with bilateral vestibular loss: a phase 1 clinical trial," *Otology & Neurotology*, Vol. 30, no. 2, pp. 210–216, 2009.

2. Ferrazzoli, D., A. Fasano, R. Maestri, R. Bera, G. Palamara, M. F. Ghilardi, G. Pezzoli, and G. Frazzitta, "Balance dysfunction in parkinson's disease: the role of posturography in developing a rehabilitation program," *Parkinson's Disease*, Vol. 2015, 2015.

3. Guemann, M., S. Bouvier, C. Halgand, F. Paclet, L. Borrini, D. Ricard, E. Lapeyre, D. Cattaert, and A. d. Rugy, "Effect of vibration characteristics and vibror arrangement on the tactile perception of the upper arm in healthy subjects and upper limb amputees," *Journal of Neuroengineering and Rehabilitation*, Vol. 16, no. 1, pp. 1–16, 2019.

4. Sandrini, G., V. Homberg, L. Saltuari, N. Smania, A. Pedrocchi, *et al.*, *Advanced Technologies for the Rehabilitation of Gait and Balance Disorders*, Vol. 19, Springer, 2018.

5. Ham, R. J., *Primary Care Geriatrics: A Case-based Approach*, Elsevier Health Sciences, 2007.

6. Horak, F. B., "Postural orientation and equilibrium: what do we need to know about neural control of balance to prevent falls?," *Age and Ageing*, Vol. 35, no. suppl_2, pp. ii7–ii11, 2006.

7. RENNIE, M., "Exercise: regulation and integration of multiple systems," *Handbook of Physiology*, pp. 995–1035, 1996.

8. Visser, J. E., M. G. Carpenter, H. van der Kooij, and B. R. Bloem, "The clinical utility of posturography," *Clinical Neurophysiology*, Vol. 119, no. 11, pp. 2424–2436, 2008.

9. Piirtola, M., and P. Era, "Force platform measurements as predictors of falls among older people–a review," *Gerontology*, Vol. 52, no. 1, pp. 1–16, 2006.

10. Gangapurwala, P., "Methods of stereophotogrammetry: A review," *Available at SSRN 3866518*, 2021.

11. Wall Iii, C., and E. Kentala, "Control of sway using vibrotactile feedback of body tilt in patients with moderate and severe postural control deficits," *Journal of Vestibular Research*, Vol. 15, no. 5-6, pp. 313–325, 2005.

12. Brugnera, C., R. S. M. Bittar, M. E. Greters, and D. Basta, "Effects of vibrotactile vestibular substitution on vestibular rehabilitation-preliminary study," *Brazilian Journal of Otorhinolaryngology*, Vol. 81, pp. 616–621, 2015.

13. Latash, M. L., *Fundamentals of Motor Control*, Academic Press, 2012.

14. Vanicek, N., S. A. King, R. Gohil, I. C. Chetter, and P. A. Coughlin, "Computerized dynamic posturography for postural control assessment in patients with intermittent claudication," *JoVE (Journal of Visualized Experiments)*, no. 82, p. e51077, 2013.

15. Rossi-Izquierdo, M., A. Ernst, A. Soto-Varela, S. Santos-Pérez, A. Faraldo-García, A. Sesar-Ignacio, and D. Basta, "Vibrotactile neurofeedback balance training in patients with parkinson's disease: reducing the number of falls," *Gait & Posture*, Vol. 37, no. 2, pp. 195–200, 2013.

16. Ballardini, G., V. Florio, A. Canessa, G. Carlini, P. Morasso, and M. Casadio, "Vibrotactile feedback for improving standing balance," *Frontiers in Bioengineering and Biotechnology*, Vol. 8, p. 94, 2020.

17. Kandel, E. R., J. H. Schwartz, T. M. Jessell, S. Siegelbaum, A. J. Hudspeth, S. Mack, *et al.*, *Principles of Neural Science*, Vol. 4, McGraw-hill New York, 2000.

18. Bordoni, B., N. L. Mankowski, and D. T. Daly, "Neuroanatomy, cranial nerve 8 (vestibulocochlear)," in *StatPearls [Internet]*, StatPearls Publishing, 2021.

19. Kauffman, T. L., J. O. Barr, and M. L. Moran, *Geriatric Rehabilitation Manual*, Elsevier Health Sciences, 2007.

20. Levangie, P. K., and C. C. Norkin, *Joint Structure and Function: a Comprehensive Analysis*, FA Davis, 2011.

21. Maeda, T., K. Ochi, K. Nakakura-Ohshima, S. Youn, and S. Wakisaka, "The ruffini ending as the primary mechanoreceptor in the periodontal ligament: its morphology, cytochemical features, regeneration, and development," *Critical Reviews in Oral Biology & Medicine*, Vol. 10, no. 3, pp. 307–327, 1999.

22. Purves, D., G. J. Augustine, D. Fitzpatrick, L. C. Katz, A.-S. LaMantia, J. O. McNamara, and S. M. Williams, "Circuits within the basal ganglia system," in *Neuroscience. 2nd Edition*, Sinauer Associates, 2001.

23. Martel, J. L., J. H. Miao, and T. Badri, "Anatomy, hair follicle," 2017.

24. Verrillo, R. T., and A. J. Capraro, "Effect of extrinsic noise on vibrotactile information processing channels," *Perception & Psychophysics*, Vol. 18, no. 2, pp. 88–94, 1975.

25. Bolanowski Jr, S., and R. T. Verrillo, "Temperature and criterion effects in a somatosensory subsystem: a neurophysiological and psychophysical study.," *Journal of Neurophysiology*, Vol. 48, no. 3, pp. 836–855, 1982.

26. Verrillo, R. T., "Investigation of some parameters of the cutaneous threshold for vibration," *The Journal of the Acoustical Society of America*, Vol. 34, no. 11, pp. 1768–1773, 1962.

27. Verrillo, R. T., "Effect of contactor area on the vibrotactile threshold," *The Journal of the Acoustical Society of America*, Vol. 35, no. 12, pp. 1962–1966, 1963.

28. Verrillo, R. T., "Effect of spatial parameters on the vibrotactile threshold.," *Journal of Experimental Psychology*, Vol. 71, no. 4, p. 570, 1966.

29. Gescheider, G. A., B. F. Sklar, C. L. Van Doren, and R. T. Verrillo, "Vibrotactile forward masking: psychophysical evidence for a triplex theory of cutaneous mechanoreception," *The Journal of the Acoustical Society of America*, Vol. 78, no. 2, pp. 534–543, 1985.

30. Gescheider, G. A., R. R. Fay, C. H. Lyons, *et al.*, "Psychophysical tuning curves in vibrotaction.," *Sensory Processes*, 1978.

31. Verrillo, R. T., and S. J. Bolanowski Jr, "The effects of skin temperature on the psychophysical responses to vibration on glabrous and hairy skin," *The Journal of the Acoustical Society of America*, Vol. 80, no. 2, pp. 528–532, 1986.

32. Capraro, A. J., R. T. Verrillo, and J. J. Zwislocki, "Psychophysical evidence for a triplex system of cutaneous mechanoreception.," *Sensory Processes*, 1979.

33. Verrillo, R. T., "A duplex mechanism of mechanoreception," in *Proc. First International Symposium on the Skin Sense, Thomas, Springfield, Illinois, 1968*, pp. 139–159, 1968.

34. Gescheider, G. A., "Evidence in support of the duplex theory of mechanoreception.," *Sensory Processes*, 1976.

35. Gescheider, G. A., *Psychophysics: the Fundamentals*, Psychology Press, 2013.

36. Verrillo, R. T., "Vibrotactile thresholds for hairy skin.," *Journal of Experimental Psychology*, Vol. 72, no. 1, p. 47, 1966.

37. Karakuş, İ., and B. Güçlü, "Psychophysical principles of discrete event-driven vibrotactile feedback for prostheses," *Somatosensory & Motor Research*, Vol. 37, no. 3, pp. 186–203, 2020.

38. Dhillon, G. S., and K. W. Horch, "Direct neural sensory feedback and control of a prosthetic arm," *IEEE Transactions on Neural Systems and Rehabilitation Engineering*, Vol. 13, no. 4, pp. 468–472, 2005.

39. Guclu, B., *Somatosensory Feedback for Neuroprosthetics*, Academic Press, 2021.

40. Cheng, L.-T., R. Kazman, and J. Robinson, "Vibrotactile feedback in delicate virtual reality operations," in *Proceedings of the Fourth ACM International Conference on Multimedia*, pp. 243–251, 1997.

41. Dixon, S., "A history of virtual reality in performance.," *International Journal of Performance Arts & Digital Media*, Vol. 2, no. 1, 2006.

42. Desai, P. R., P. N. Desai, K. D. Ajmera, and K. Mehta, "A review paper on oculus rift-a virtual reality headset," *ArXiv Preprint ArXiv:1408.1173*, 2014.

43. O'Neil, C., M. D. Dunlop, and A. Kerr, "Supporting sit-to-stand rehabilitation using smartphone sensors and arduino haptic feedback modules," in *Proceedings of the 17th International Conference on Human-Computer Interaction with Mobile Devices and Services Adjunct*, pp. 811–818, 2015.

44. Brock, J. D., R. F. Bruce, and S. L. Reiser, "Using arduino for introductory programming courses," *Journal of Computing Sciences in Colleges*, Vol. 25, no. 2, pp. 129–130, 2009.

45. "Arduino UNO Rev3 kernel description." https://store.arduino.cc/products/arduino-uno-rev3?queryID=undefined. Accessed: 2022-07-15.

46. Rasheed, A. S., R. H. Finjan, A. A. Hashim, and M. M. Al-Saeedi, "3d face creation via 2d images within blender virtual environment," *Indonesian Journal of Electrical Engineering and Computer Science*, Vol. 21, no. 1, pp. 457–464, 2021.

47. Ebert, D., V. Metsis, and F. Makedon, "Development and evaluation of a unity-based, kinect-controlled avatar for physical rehabilitation," in *Proceedings of the 8th ACM International Conference on PErvasive Technologies Related to Assistive Environments*, pp. 1–2, 2015.

48. Tsumaki, Y., H. Naruse, D. N. Nenchev, and M. Uchiyama, "Design of a compact 6-dof haptic interface," in *Proceedings. 1998 IEEE International Conference on Robotics and Automation (Cat. No. 98CH36146)*, Vol. 3, pp. 2580–2585, IEEE, 1998.

49. Chen, C.-H., M.-C. Jeng, C.-P. Fung, J.-L. Doong, and T.-Y. Chuang, "Psychological benefits of virtual reality for patients in rehabilitation therapy.," *Journal of Sport Rehabilitation*, Vol. 18, no. 2, 2009.

50. Gibby, J. T., S. A. Swenson, S. Cvetko, R. Rao, and R. Javan, "Head-mounted display augmented reality to guide pedicle screw placement utilizing computed tomography," *International journal of Computer Assisted Radiology and Surgery*, Vol. 14, no. 3, pp. 525–535, 2019.

51. Kipman, A., "Eth global lecture series: Hololens 2 - unpacked," 2019.

52. E-komponent, "Dc motor vibration, erm 10000 rpm 3vdc," 2022.

53. Madigan, M. L., B. S. Davidson, and M. A. Nussbaum, "Postural sway and joint kinematics during quiet standing are affected by lumbar extensor fatigue," *Human Movement Science*, Vol. 25, no. 6, pp. 788–799, 2006.

54. Van Wyk, E., and R. De Villiers, "Virtual reality training applications for the mining industry," in *Proceedings of the 6th International Conference on Computer Graphics, Virtual Reality, Visualisation and Interaction in Africa*, pp. 53–63, 2009.

55. Jacobson, J., M. S. Redfern, J. M. Furman, S. L. Whitney, P. J. Sparto, J. B. Wilson, and L. F. Hodges, "Balance nave: a virtual reality facility for research and rehabilitation of balance disorders," in *Proceedings of the ACM Symposium on Virtual Reality Software and Technology*, pp. 103–109, 2001.

56. Lee, B.-C., B. J. Martin, and K. H. Sienko, "Directional postural responses induced by vibrotactile stimulations applied to the torso," *Experimental Brain Research*, Vol. 222, no. 4, pp. 471–482, 2012.

57. Sienko, K. H., M. D. Balkwill, L. I. Oddsson, and C. Wall, "The effect of vibrotactile feedback on postural sway during locomotor activities," *Journal of Neuroengineering and Rehabilitation*, Vol. 10, no. 1, pp. 1–6, 2013.

58. Nanhoe-Mahabier, W., J. Allum, E. Pasman, S. Overeem, and B. Bloem, "The effects of vibrotactile biofeedback training on trunk sway in parkinson's disease patients," *Parkinsonism & Related Disorders*, Vol. 18, no. 9, pp. 1017–1021, 2012.

59. Ho, N., P.-M. Wong, M. Chua, and C.-K. Chui, "Virtual reality training for assembly of hybrid medical devices," *Multimedia Tools and Applications*, Vol. 77, no. 23, pp. 30651–30682, 2018.

APPENDIX A. ADDITIONAL TABLES

A.1 Tables

Table A.1
Threshold values of the anterior motion detection experiment at 4 different speed.

	2dgs	1.5dgs	1dgs	.5dgs
Thresholds (deg):	0,028	0,027	0,027	0,037

Table A.2
Threshold values of the posterior motion detection experiment at 4 different speed.

	2dgs	1.5dgs	1dgs	.5dgs
Thresholds (deg):	0,0251	0,026	0,0253	0,038

Table A.3
Correct classification numbers of the angle discrimination task for the anterior sway.

Additional Angles	Reference Angles		
	90.5 deg	92.0 deg	93.5 deg
0.05 deg	10/20	10/20	9/20
0.1 deg	13/20	12/20	11/20
0.15 deg	14/20	10/20	10/20
0.2 deg	16/20	15/20	16/20
0.35 deg	15/20	17/20	14/20
0.5 deg	18/20	14/20	17/20
2 deg	17/20	20/20	19/20
3.5 deg	20/20	20/20	18/20

Table A.4
Correct classification numbers of the angle discrimination task for the posterior sway.

Additional Angles	Reference Angles		
	89.5 deg	88.0 deg	86.5 deg
0.05 deg	9/20	12/20	11/20
0.1 deg	9/20	15/20	8/20
0.15 deg	10/20	11/20	14/20
0.2 deg	14/20	13/20	15/20
0.35 deg	15/20	15/20	16/20
0.5 deg	17/20	15/20	15/20
2 deg	20/20	20/20	20/20
3.5 deg	20/20	20/20	20/20

Table A.5
Shows the correct answer classification numbers of the Velocity discrimination task for the anterior sway.

Additional velocities	Reference Velocity (deg/s)		
	1	2	3
0.1	11/20	9/20	7/20
0.2	17/20	13/20	10/20
0.3	17/20	16/20	16/20
0.4	19/20	18/20	18/20
0.5	19/20	20/20	20/20

Table A.6
Shows the correct answer classification numbers of the Velocity discrimination task for the posterior sway.

Additional velocities	Reference Velocity (deg/s)		
	1	2	3
0.1	12/20	8/20	9/20
0.2	16/20	11/20	13/20
0.3	18/20	15/20	12/20
0.4	18/20	19/20	18/20
0.5	20/20	20/20	20/20

Table A.7
Detailed precision, recall, f1, and accuracy scores of single pulse mixed modulated vibrotactile stimuli localization.

	Precision	Recall	F1-score	Number
Class1	0.56	1	0.71	20
Class2	0.56	0.45	0.5	20
Class3	0.7	0.35	0.47	20
Class4	1	0.95	0.97	20
Class5	0.83	0.75	0.79	20
Class6	0.81	0.85	0.83	20
Avg	0.74	0.72	0.71	120
Accuracy	0.73			120

Table A.8
Detailed precision, recall, f1, and accuracy scores of double pulse mixed modulated vibrotactile stimuli localization.

	Precision	Recall	F1-score	Number
Class1	0.83	1	0.91	20
Class2	0.62	0.65	0.63	20
Class3	0.86	0.6	0.71	20
Class4	0.91	1	0.95	20
Class5	0.75	0.90	0.82	20
Class6	0.87	0.65	0.74	20
Class7	0.80	1	0.89	20
Class8	0.65	0.75	0.7	20
Class9	0.92	0.6	0.73	20
Class10	1	0.85	0.92	20
Class11	0.75	0.9	0.82	20
Class12	0.89	0.8	0.84	20
Avg	0.82	0.81	0.8	240
Accuracy	0.81			240

Table A.9
Detailed precision, recall, f1, and accuracy scores of pulse-number modulated vibrotactile stimuli localization (4/10 pulse).

	Precision	Recall	F1-score	Number
Class1	0.76	0.95	0.84	20
Class2	0.82	0.7	0.76	20
Class3	0.94	0.8	0.86	20
Class4	0.76	0.95	0.84	20
Class5	0.67	0.8	0.73	20
Class6	1	0.65	0.79	20
Class7	0.83	0.95	0.88	20
Class8	0.79	0.75	0.77	20
Class9	0.94	0.85	0.89	20
Class10	0.91	1	0.95	20
Class11	0.65	0.85	0.74	20
Class12	0.91	0.5	0.65	20
Avg	0.83	0.81	0.81	240
Accuracy	0.81			240

Table A.10
Detailed precision, recall, f1, and accuracy scores of pulse-number modulated vibrotactile stimuli localization (4/7/10 pulse).

	Precision	Recall	F1-score	Number
Class1	0.83	0.95	0.88	20
Class2	0.44	0.4	0.42	20
Class3	0.75	0.45	0.56	20
Class4	1	0.7	0.82	20
Class5	0.89	0.85	0.87	20
Class6	0.89	0.85	0.87	20
Class7	0.71	0.85	0.77	20
Class8	0.54	0.7	0.61	20
Class9	0.67	0.6	0.63	20
Class10	0.73	0.8	0.76	20
Class11	0.68	0.85	0.76	20
Class12	0.67	0.8	0.73	20
Class13	0.85	0.85	0.85	20
Class14	0.57	0.4	0.47	20
Class15	0.56	0.7	0.62	20
Class16	0.85	0.85	0.85	20
Class17	0.95	1	0.98	20
Class18	1	0.8	0.89	20
Avg	0.75	0.74	0.74	360
Accuracy	0.74			360

Table A.11
Detailed precision, recall, f1, and accuracy scores of incrementally recruited pulse-number modulated vibrotactile stimuli training for anterior motors(4/10 pulse).

	Precision	Recall	F1-score	Number
Class1	1	1	1	20
Class2	0.83	1	0.91	20
Class3	1	0.8	0.89	20
Class4	1	1	1	20
Class5	0.86	0.95	0.9	20
Class6	0.94	0.85	0.89	20
Avg	0.94	0.93	0.93	120
Accuracy	0.93			120

Table A.12
Detailed precision, recall, f1, and accuracy scores of incrementally recruited pulse-number modulated vibrotactile stimuli training for posterior motors(4/10 pulse).

	Precision	Recall	F1-score	Number
Class1	1	1	1	20
Class2	0.78	0.9	0.84	20
Class3	0.88	0.75	0.81	20
Class4	1	1	1	20
Class5	0.86	0.95	0.9	20
Class6	0.94	0.85	0.89	20
Avg	0.91	0.91	0.91	120
Accuracy	0.91			120

Table A.13
Detailed precision, recall, f1, and accuracy scores of visual avatar identification for anterior sway.

	Precision	Recall	F1-score	Number
Class1	0.95	1	0.95	95
Class2	0.82	0.9	0.86	20
Class3	0.94	0.85	0.89	20
Class4	0.87	1	0.93	20
Class5	0.94	0.85	0.89	20
Class6	1	0.95	0.97	20
Avg	0.92	0.92	0.92	120
Accuracy	0.92			120

Table A.14
Detailed precision, recall, f1, and accuracy scores of visual avatar identification for posterior sway.

	Precision	Recall	F1-score	Number
Class1	1	0.9	0.95	20
Class2	0.71	0.85	0.77	20
Class3	0.83	0.75	0.79	20
Class4	1	0.95	0.97	20
Class5	0.91	1	0.95	20
Class6	1	0.95	0.97	20
Avg	0.91	0.90	0.90	120
Accuracy	0.90			120